

Received March 17, 2020, accepted March 31, 2020, date of publication April 6, 2020, date of current version April 23, 2020.

Digital Object Identifier 10.1109/ACCESS.2020.2986010

On Modeling Optimizations and Enhancing Routing Protocols for Wireless Multihop Networks

FAHAD AHMAD AL-ZAHRANI 

Computer Engineering Department, Umm Al-Qura University, Mecca 24381, Saudi Arabia

e-mail: fayzahrani@uqu.edu.sa

The work was funded by grant number 12-INF2970-10 from the National Science, Technology and Innovation Plan (MAARIFAH), the King Abdul-Aziz City for Science and Technology (KACST), Kingdom of Saudi Arabia, and the Science and Technology Unit at Umm Al-Qura University for their continued logistics support.

ABSTRACT The contribution of this paper is two fold. It first analyses the flooding strategies for the Wireless Multihop Networks (WMNs) then it enhances the reactive and proactive routing protocols. For analysis purpose, we select four widely used flooding techniques for routing: i. traditional flooding, ii. Time-To-Live based Expanding Ring Search (*TTL*-based ERS) flooding scheme, iii. *TTL*-based Scope Routing (SR) flooding and iv. Multi-Point Relays (MPR) flooding. These techniques play a vital role and act as a backbone for routing protocols. Therefore, we compare efficiency of these techniques for six widely used routing protocols: Ad-hoc On-demand Distance Vector (AODV), Destination Sequenced Distance Vector (DSDV), Dynamic Source Routing (DSR), DYnamic MANET On-demand (DYMO), Fish-eye Scope Routing (FSR) and Optimized Link State Routing (OLSR). DSDV uses traditional flooding, AODV, DSR and DYMO use *TTL*-based ERS flooding, FSR uses *TTL*-based SR flooding and OLSR uses MPR flooding. This paper also presents mathematical models for flooding techniques and studies the affects of these techniques on their respective protocols in terms of energy and time consumption. This is done to measure the cost incurred by the routing protocols in the form of routing overhead and latencies. A novel contribution of this work is the enhancement in search set values and intervals of routing algorithms to improve the efficiency of selected existing protocols. A detailed comparison analysis of selected protocols with their default and enhanced routing algorithms in NS-2 is also a part of this work.


INDEX TERMS Time-To-Live, expanding ring, destination sequenced distance vector, DYnamic MANET On-demand, ad-hoc on-demand distance vector, wireless multihop networks.

I. INTRODUCTION

Wireless Multihop Networks (WMNs) are the type of wireless networks that use multi-hop routing mechanism for communication. A mobile user with wireless node in WMNs can indirectly communicate on the move with other mobile users. Hence, routing protocols play a major part in providing and maintaining an indirect communication path between all mobile users that are part of this fully dynamic and distributed network. Different routing protocols are proposed that adapt varying techniques to search and maintain suitable path(s) between source(s) and destination(s). Moreover, routing strategies of these protocols are aimed to minimize

both the overhead and the convergence time for the dynamic topology of WMNs.

In WMNs, a route towards the destination is found by disseminating the route request messages. Upon reception, the destination sends the route reply message as a reply to the originator of route request. Various techniques have been proposed to propagate these responses throughout the network. Most widely used mechanism is the *traditional/complete flooding* or simply *flooding*. In traditional flooding strategy, the originator sends route request message to its nearest entities, which forward these requests further to their nearest entities until the message is successfully delivered to the destination node. The traditional flooding technique has very high route searching control overhead in WMNs. Due to high control overhead in traditional flooding strategy, several other

The associate editor coordinating the review of this manuscript and approving it for publication was IlSun You .

techniques have been proposed to minimize the overhead that include *Time-To-Live (TTL)*-based and *Node Degree*-based strategies [1].

In *TTL*-based strategy, flooding of route request message is confined within the specified region by assigning the value of *TTL*. The *TTL* value is fixed by the originator of request packet and is carried out in the route request packet. Each time when the request packet is relayed, a decrease in *TTL* value is observed. This process continues until value of *TTL* becomes zero and propagation of request packet stops. As a result, broadcast area of request message is governed by the *TTL* value. The destination node replies to the request only if it is within a specified region. Otherwise, source node restarts the search again with larger *TTL* value than the previous one. This process continues until the destination node is found or the originator gives up. On the other hand, in node degree based strategy, the source node selects a small subset of its neighboring nodes that are responsible to forward the request message. Similarly, each node within that subset selects another subset of forwarding nodes from its neighbors and continues relaying request message. This strategy also minimizes the flooding control overhead. However, computation of the optimal local subset is quite difficult in the case of WMNs.

This paper presents an empirical model of the above said routing strategies along with the routing protocols that employ these techniques. To evaluate these strategies, we select six widely used routing protocols, which are: Ad-hoc On-demand Distance Vector (AODV) [2], Destination Sequence Distance Vector (DSDV) [3], Dynamic Source Routing (DSR) [4], DYNAMIC MANET On-demand (DYMO) [5], Fish-eye Scope Routing (FSR) [6] and Optimized Link State Routing (OLSR) [7]. This work also contributes in terms of enhancing the efficiency of the selected routing protocols in the form of Normalized Routing Load (NRL) and reduced latencies. In addition, a mathematical model is presented to give critical analysis of the existing work. Further, the addition of *NRL* in existing schemes show significant improvements in terms of throughput and delay. It is worth mentioning that this study has been conducted by inspiring from [8]–[11] and [12]. The comparison of the performance of the selected routing protocols is done by simulating them in NS-2 environment. The efficiency is compared in terms of *throughput*, End-To-End Delay (*E2ED*) and (*NRL*).

Rest of the paper is arranged in the following manner. Section II provides insights about the previous work related to the topic. The empirical models of traditional flooding, routing protocols that employ this flooding strategy and their necessary enhancements are briefly discussed in section III. Similarly, the empirical models of *TTL*-based and degree based routing strategies along with the routing protocols that adapt these schemes are discussed in section IV and section V, respectively. Simulation results of the conventional routing protocol models with default parameters and

the proposed empirical models with enhanced parameters are discussed in section VI. Finally, section VII concludes the paper.

II. RELATED WORK

Flooding provides multipath diversity and is considered a promising approach for routing. Authors in [13] presented a flooding based routing protocol (REALFLOW) for Industrial Wireless Sensor and Actuator Networks (IWSANs). The REALFLOW provides enhanced network stability and reliability when compared against four traditional flooding based protocols, which are: Normal flooding, Location flooding, Directional flooding and Single Gossiping with Directional Flooding (SGDF) in terms of packet delivery ratio within deadlines, consecutive packet loss and total packet transmissions.

Authors in [14], propose a protocol based on the selective-path priority table for the deployment of the mobile sink. Two short routes leading towards the cluster head or sink node are prioritised to make the priority table using the simple and effective rules. Rules are developed using the defined transmission and residual energy metrics. An energy-efficient routing protocol for prolonging network lifetime is presented in [15], which is referred to as Balancing Ant-based Routing Algorithm (EBAR). It uses the pseudo-random path searching algorithm along with the enhanced pheromone updating approach for balancing the energy consumption of the sensors. The results of this approach show that it has improved the lifetime and energy efficiency of the system as compared the previous schemes.

Radwan, A. A. *et al.* in [16] presented a detailed comparison of the major characteristics of AODV, FSR and Location-Aided Routing (LAR) protocols to analyze control overhead, *throughput* and *E2ED* using *GloMoSim*. They deduced from simulation results that FSR has low control overhead as compared to AODV and LAR, whereas AODV has high *throughput* in comparison with rest of the protocols. Moreover, LAR has low routing delay as compared to FSR and AODV protocols.

The work in [17] describes the multi-path routing scheme for underwater sensor networks. The purpose of this scheme is to monitor the nodes having the higher energy efficiency along with the packet delivery ratio, which is validated through the simulations. Simulation results also demonstrate that this scheme has improved the end to end delay, energy efficiency and packet delivery ratio as compared to the previous schemes. Various challenges, i.e., low throughput, short life cycle and other energy constraints of the nodes in a network are tackled by the K-means and fuzzy analytic hierarchy process [18]. Where, clustering is done by the K-means algorithm in the network and cluster head selection is done by the fuzzy analytic hierarchy process based on the considered factors in the system. This system was designed for improving the life cycle of the nodes while reducing the energy consumption.

In [19], route discovery using AODV routing protocol with directional antennas is performed. The proposed technique implements AODV routing protocol to transmit data from boarder node to the gateway node. When compared against existing CR-AODV (Cognitive Radio-AODV) routing protocol, the proposed technique performed better in utilizing the network energy consumption resulting in high data delivery.

In [20], performance of a reactive routing strategy is compared against Many-to-one Deliverability of Greedy Routing (MDGR). Link collision and congestion severely affect performance of greedy routing. In order to provide reliable characterization of data deliver-abilities, authors conducted a detailed analysis to measure the effects of link collision and network congestion in 2D wireless networks. Simulation results proved the correctness of the derived upper bound on critical transmission power.

A twofold problem is resolved in [21], where, traffic routing and security-based functions' activations are discussed in the multi-hop networking environment. Total energy of the nodes is reduced, and their security demand are also fulfilled. Authors in [22] discuss the movement of the mobile sink around the tracking region. It acts as an original source node in this region. There is an issue of flooding, when different nodes send the packets at the same time. So, this scheme addresses the issue related to the flooding and validated it to prove the system effectiveness. Its results show that flooding delay is minimized. In multi-hop networks, it is very difficult to compute the packet-level routing [23]. This information is very beneficial in the activities like managing the networks. Authors have addressed this path reconstruction issue using various algorithms and proved their effectiveness by performing simulations.

Authors in [12] proposed a detailed framework for reducing routing overhead. The control overhead for route maintenance operation of chosen protocols: *plain flooding* of DSDV, *Multi-Point Relays (MPRs) flooding* in OLSR and *Fish-eye scope* routing of FSR, is modeled according to appropriate computed probabilities. This further includes: change in MPRs, neighbor discovery error and number of link breakages.

Sinha et al. [24] proposed a dynamic multi hop broadcast routing protocol for emerging wireless networks. Tight upper and lower bounds on broadcast capacity are defined to improve the network throughput. The exponential growth of the spanning trees proved to be inefficient for the broadcast in topologies exhibiting the spanning trees. Therefore, this paper used adaptive broadcast techniques to improve the network throughput.

Kuang et al. [25] proposed a bandwidth based multi-hop WSN for real-time information sharing. When a node requests for the required content, there may exist multiple information provider nodes. So, in order to select an information provider, the distance and available path size is checked. An information provider with a wider path and the shortest distance is selected to send the required content to the requester.

Authors in [26] provided a comparative analysis of two routing protocols: RPL and thread. Form a detailed analysis of both protocols it is concluded that the thread routing protocol is better and it efficiently provides connectivity between low powered devices over a multihop WSN. However, in terms of scalability, the RPL routing protocol is better.

In paper [27], the authors focused on maximizing the throughput of the multicast traffic pattern in MWN using the Time Division Multiple Access (TDMA) approach. The authors generalized minimum frame length problem for multicast traffic from a single source to multiple destinations. This non-trivial characteristic of the proposed generalization mechanism makes it mathematically untrackable and computationally complex as compared to its unicast counterpart. In the proposed work, the concept of unicast compatible sets is extended to a multicast scenario using the Mixed Integer Programming (MIP) technique for an arbitrary network, where packets transmitted from each transmitter are received at different subsets of receivers. Authors used the linear relaxation of MIP, multicast tree optimization and compatible set generation to solve the optimization problem. Furthermore, different length packets, multiple modulation technique and usage of different coding schemes for delay minimization are also included in the proposed work.

Route discovery is an indispensable process for successful data sharing between leaf nodes and sink nodes. Therefore, broadcasting is widely used in literature for path finding. In [28], the authors proposed a customized proactive routing strategy to achieve energy efficiency in clustered Internet of Things Wireless Sensor Networks (IoT-WSNs). The simulation results of the proposed strategy proved that it outperformed existing strategies, in terms of maximized throughput and network lifetime.

In [29], the authors proposed a selective multipath routing protocol based on their first protocol named as Multipath-ChaMeLeon (M-CML) for ubiquitous network. The proposed protocol is named as M-CMLv2, in which authors considered three different Quality of Service (QoS) metrics and performed the network optimization analysis with statistical significance. To enhance the effectiveness of the M-CML, an intelligent algorithm is applied to reduce the improvident emission of packets. Different performance evaluation metrics like E2ED, NRL, packet delivery ratio, energy consumption and redundant packet suppression are compared for OLSR, AOMDV and M-CML using the NS-3 simulator. The simulation results showed that the M-CMLv2 reduced the redundant information and delivered packets successfully with acceptable E2ED. It also reduced NLR and the energy consumption of the nodes.

A cross technology communication routing protocol is proposed in [30]. This protocol uses Wi-Fi to transmit data over long distances and assists the ZigBee embedded devices. To establish a routing path, the Wi-Fi nodes send the bacon messages to the ZigBee embedded devices to awake them. The experimental results exhibit the effectiveness of

the proposed routing protocol to establish communication between cross technology devices.

An optimized clustering and energy efficient routing protocol for mobile nodes in WSNs is proposed in [31]. A clustering algorithm is executed in a centralized manner and clusters of moving nodes are made. If a node is disconnected from a cluster it automatically connects with another nearby cluster head by calculating the distance. The objective of this routing protocol is to achieve the energy efficiency of nodes while sharing maximum data.

Authors in [32] provided a comparative analysis of ZigBee topologies for wireless lighting control system. These topologies are tested using two routing protocols: AODV and DSR. The comparison shows that end to end delay is minimum when DSR is implemented on start topology. However, it suffers from the problem of the center point of failure. On the other hand, mesh topology with the same routing protocol also emerged as a promising solution if the system is not time critical.

In [33] authors have proposed a mode selection mechanism for frequency division duplex nodes. These nodes are divided into two groups according to their frequency bands of data transmission and reception. In the proposed work, the nodes select their frequency band in such a way that each node can communicate with all other nodes, of the same network, present at its one hop. The bipartite graph coloring scheme is used for mode selection and simulation results depict the effectiveness of the proposed scheme.

Authors in [34] highlight the deficiency of an underlay network that it is designed without considering the importance of what a user of this network wants. Considering the importance of a user's preferences, authors propose a framework of a multihop network. They have also designed an interface, which transforms technical terms into non-technical terms so that an average user can easily understand it. The simulations depict that the proposed framework successfully achieves the objective of this work.

In [35], a lightweight countermeasure to cater the selective forwarding attached in WSNs is designed, analyzed and evaluated. A randomly deployed single checkpoint node is selected to detect the misbehaving forwarding node. Whereas, the proposed approach is used for both timeout and hop-by-hop based retransmission approaches, to recover the lost packets. The authors also considered the false detection and analyzed the false detection rate using the checkpoint node.

The authors in paper [36] proposed a computationally effective Receiver Based Flooding (RBF) algorithm for Mobile Adhoc Networks (MANETs). In the proposed work, the authors focused on reducing complexity and redundancy during transmission of packets. The computational complexity of the proposed RBF algorithm is $O(n \log n)$ compared with the $O(n^2)$ of the conventional RBF schemes. Further, the RBF scheme is extended to RBF-E1 and RBF-E2. The former shows good performance when the defer time is short; while, the latter reduces the complexity to $O(n)$.

A dynamic topology resilient smart world routing protocol is proposed by Biswas, P. K. *et al.* [37]. The goal was to find an efficient route towards destination. It selects a data forwarder, which is closest to the final destination. Simulation results show minimum E2ED and packet loss ratio when compared against existing counterpart schemes.

In [38], the authors conducted a comprehensive survey about the integration of opportunistic routing and interflow network coding. Comparison of several joint routing protocols like Interflow NC with Opportunistic Routing (XCOR), Coding-Aware Opportunistic Routing (CAOR), Active Network Coding High-throughput Optimizing Routing (ANCHOR) etc. is provided along with their pros and cons.

Authors in [39] provided a comprehensive analysis of the stateless geographic routing protocol's performance in three dimensional Flying Ad-hoc Networks (FANETs). This routing strategy exploits the location information of nodes using greedy forwarding. Performance of the proposed work is compared against state-of-the-art in geographic routing.

During the past few decades the use of Unmanned Aerial Vehicles (UAVs) in MANETs has been emerged. However, the authors in [40] identified that the exiting protocols do not work well for UAVs. This article focuses on the route establishment for UAVs and identifies open research problems. According to the authors of this paper, the routing protocols for UAVs are categorized into two major categories i.e. Single hop routing and multi hop routing. Some of the proactive, reactive and hybrid protocols are also discussed under the heading of multi hop routing. Dijkstra's algorithm has been used by [41] to find optimal routing path in Adhoc networks. This work optimizes the transmit power and secure routes to derive the routing weights.

In [42], the authors proposed a bandwidth-satisfied and coding-aware multicast routing protocol (BCMRP). The scheme uses distributed hash table for reliable communication in partition based ad hoc networks. According to this study, mobility of the node and their limited transmission range can cause network partitioning in ad hoc networks. This partitioning may result in inaccessibility of certain nodes. This work intelligently avoids the problem of pre-partitioning.

Cooperative communication is appealing because of its flexibility in MANETs. A constructive relay based protocol is proposed by using the topological information and maintaining two types of tables (relay table and cooperative table) [43]. Two types of routing problems: frequent link breakage and quick energy exhaustion are also taken into consideration.

Routing is a process of finding path(s) between source node(s) (S_n) and destination node(s) (D_n) to carry out communication. In this process, there may be n relay node(s) R_n , while connecting S_n with D_n . Routing protocols are categorized based on the routing methods they employ, as well as the processes used to find and maintain paths in the network. In this work, we characterized routing protocols based on

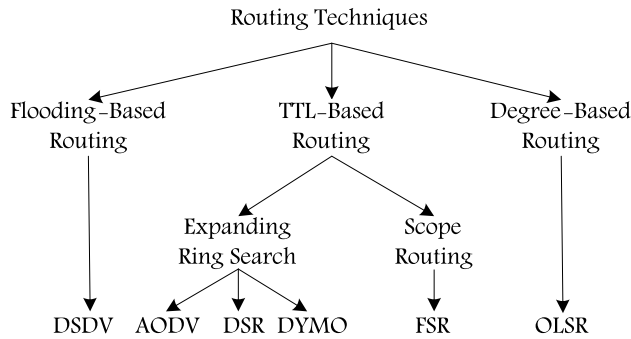


FIGURE 1. Routing techniques used by routing protocols.

routing strategies they adopt to perform routing tasks; Traditional Flooding, *TTL*-based Expanding Ring Search (ERS) and SR and MPRs or node degree based routing technique, as shown in fig. 1. Before connecting the empirical model of the above said routing strategies along with their employing routing protocols, we make the generalized empirical model for Cost of Energy (*CE*) and Cost of Time (*CT*) parameters. The reason to model *CE* and *CT* first is that we will evaluate empirical models of routing strategies based on these two parameters. During evaluation, we use different search set values (k_i) to analyze their effect on *CE* and *CT* generated by the routing strategies. Following sections discuss the detailed model of the above said routing strategies; flooding-based routing, *TTL*-based routing, and degree-based routing for the chosen protocols.

III. FLOODING-BASED ROUTING STRATEGY

In flooding based routing strategy, route search which leads to D_n , where n is the intermediate hop which is involved in delivering the data at the destination (from now on we use the term search instead of route search to D_n) is performed throughout the network, N . To find D_n , S_n initiates search based on search set value k_i (the number of hops i.e., *TTL*), where i shows the broadcast region in which search is performed. Let, k_N denotes the network diameter (predefined value of N be 255), and thus *TTL* value of k_i be set up to N . In this case, whole network is flooded with route search control packets to find route(s) to D_n .

In MANET, the nodes which are located in the range are capable to communicate directly with S_n ; called adjacent or neighboring nodes. The total number of directly connected or neighboring nodes depicts the node degree (d). An isolated node has zero degree. Let, $d_{avg}^{(k_N)}$ be an average node degree of each node in the MANET, then the degree of connectivity for that node with its first hop neighbors, called expected forward degree, of that node is; d_f . Here, nodes with higher degree d_f forward received broadcast message with certain probability of success, P_s [44]. In flooding based technique, S_n initiates the search by broadcasting route request packet. This control packet is received by d and further disseminated by d_f with P_s in MANET until D_n receives that packet.

The detailed steps of traditional flooding strategy are shown in algorithm 1 and well depicted in fig. 2. In fig. 2, S_n is

connected with 8 nodes, therefore, its $d_f = 8$. For k_2 in fig. 2, each adjacent first hop neighbor of source node is connected with d of 4, therefore, d_f for k_2 is 4 and so on. As *TTL* value of last k_i is zero (as process of forwarding continues till k_{N-1} search set and stops at k_N). Therefore, d_f of k_N becomes zero. The routing control overhead of the above discussed traditional flooding in terms of *CE*, $CE_{flooding}^{k_N}$, is computed using equation 1, taken from [12].

$$CE_{flooding}^{k_N} = P_s d_{avg}^{k_N} + d_{avg}^{k_N} \sum_{i=1}^{k_N-1} (P_s)^{i+1} \prod_{j=1}^i d_f^{k_N}[j] \quad (1)$$

where, $d_{avg}^{(k_N)}$ is calculated using equation 2, taken from [12].

$$d_{avg}^{k_N} = \frac{1}{k_N} \sum_{i=1}^{k_N} d_f[i] \quad \text{for flooding} \quad (2)$$

Algorithm 1 Traditional Flooding

- 1: **begin**
 - 2: $S_n \leftarrow$ source node
 - 3: $msg \leftarrow$ requested message
 - 4: *TTL_VALUE* of $msg \leftarrow$ 255 hops
 - 5: S_n broadcast msg
 - 6: $R_n \leftarrow$ receiver of msg
 - 7: **for all** R_n **do**
 - 8: **if** already process msg **then**
 - 9: do not broadcast msg
 - 10: **else**
 - 11: *TTL_VALUE* \leftarrow *TTL_VALUE* - 1
 - 12: **if** (*TTL_VALUE*=0) **then**
 - 13: discard msg
 - 14: **else**
 - 15: R_n broadcast msg
 - 16: **end if**
 - 17: **end if**
 - 18: **end for**
 - 19: **end**
-

This flooding strategy has been adopted by different routing protocols e.g. DSDV, AODV, DSR and OLSR to perform route search in MANETs. However, in this work we have selected DSDV [3] to examine the behavior of flooding and section III-A is devoted to discuss it in detail.

A. ORIGINAL DSDV (DSDV-ORIG)

DSDV [3] is one of the proactive routing protocols that uses traditional flooding mechanism to perform search and maintain topological information in the Routing Table (RT). Three different operations are performed by DSDV to maintain RT. These operations include; (1) Periodic Link Status Monitoring (LSM_{Per}), (2) Trigger Route Update (RU_{Tri}) and, (3) Periodic Route Update (RU_{Per}), as shown in fig. 3(a) and fig. 4(a); inspired from [8]. LSM_{Per} maintains a record of latest and updated information about Link Status (*LS*) in the network. Moreover, it also verifies the connectivity of the

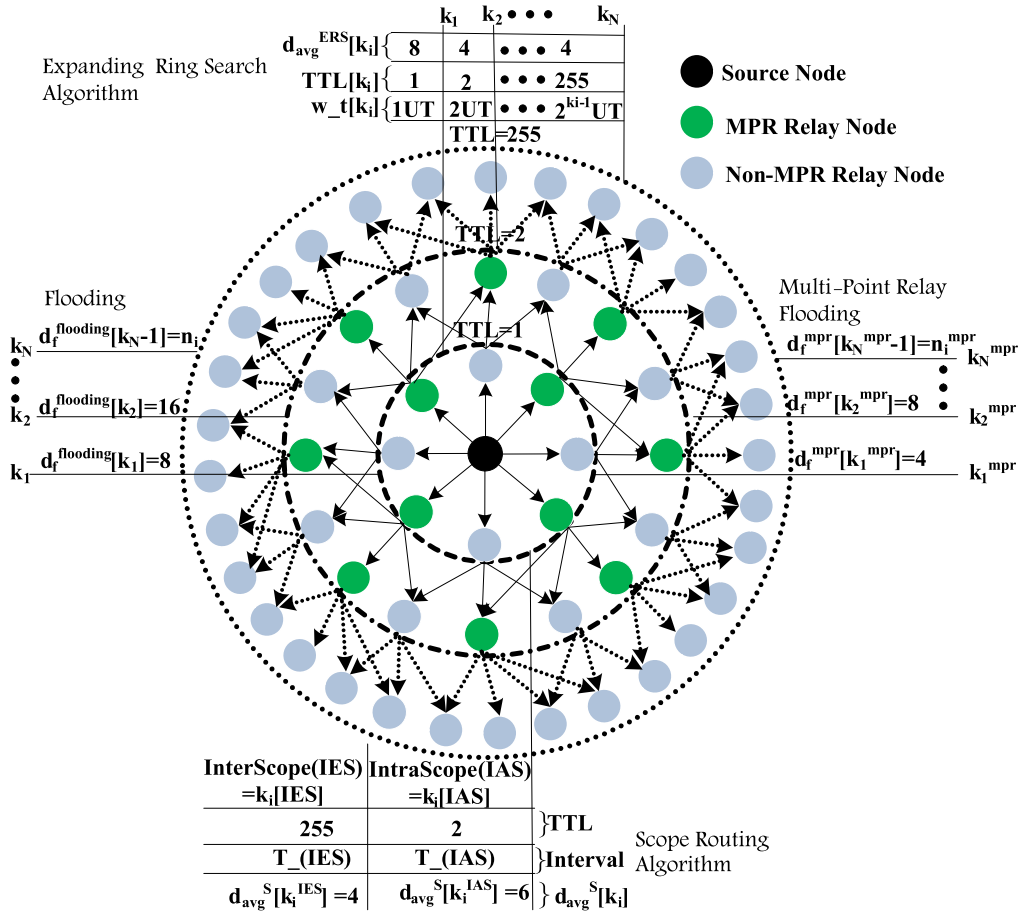


FIGURE 2. Flooding strategy.

nodes present in the network. DSDV relies on the notification of beacon message from MAC layer to maintain connectivity information. This notification is based on the principle that if a node does not receive any beacon message from its neighbor for many successive beacon intervals, then the link is assumed to be broken. RU_{Per} operation updates routing information across the network after a constant time interval and is known as *full dump* period.

The changes of LS occur in an Active Route (AR) state and RU_{Tri} are flooded throughout the network to disperse the updates across the network (fig. 4(a)). Unlike RU_{Per} , all link changes in a specified time interval are gathered by this function, before broadcasting the route updates in the network. The RU_{Tri} operation may appear to be redundant along with the LSM_{Per} operation. However, it has a certain benefit i.e., avoidance of routing loops. On the contrary, RU_{Per} includes dispersion of destination sequence numbers throughout the network, which help in monitoring and maintaining liveliness of the routing information. Moreover, LSM_{Per} operation is performed to eliminate the routing loops from the network using the latest sequence numbers.

To reduce routing overhead in flooding, DSDV uses Network Protocols Data Units (NPDUs) to transmit updates

and carry distance vector information, as shown in Fig.3. RU_{Tri} 's are transmitted using single NPDU after *incremental dump* period, which depends on the link breakage notification among ARs. Whereas, after *full dump* period, RU_{Per} are transmitted through single or multiple NPDU(s) depending on the size of changes in RT entries from the last *full dump* period. A single *InterScope_Interval* is sufficient to broadcast the routing information throughout MANET, which is neither dense nor dynamic. Whereas, in a highly dynamic environment, RT information is broadcasted in multiple NPDUs for RU_{Per} .

To achieve quality routing, a specific amount is incurred by the routing protocol (rp), denoted as: $C_{total}^{(rp)}$. This amount is in terms of energy consumption for transmitting routing control packets (CE) and time spent for routing (CT) and is computed using equation 3 [12].

$$C_{total}^{(rp)} = CE^{(rp)} \times CT^{(rp)} \quad (3)$$

In case of DSDV, let $CE_{total}^{(DSDV)}$ be the total cost for DSDV on network layer. As, DSDV transmits RU_{Tri} and RU_{Per} on network layer; therefore, $CE_{total}^{(DSDV)}$ is the sum of energy consumed by RU_{Per} ; $CE_{Per}^{(DSDV)}$ and energy consumed to

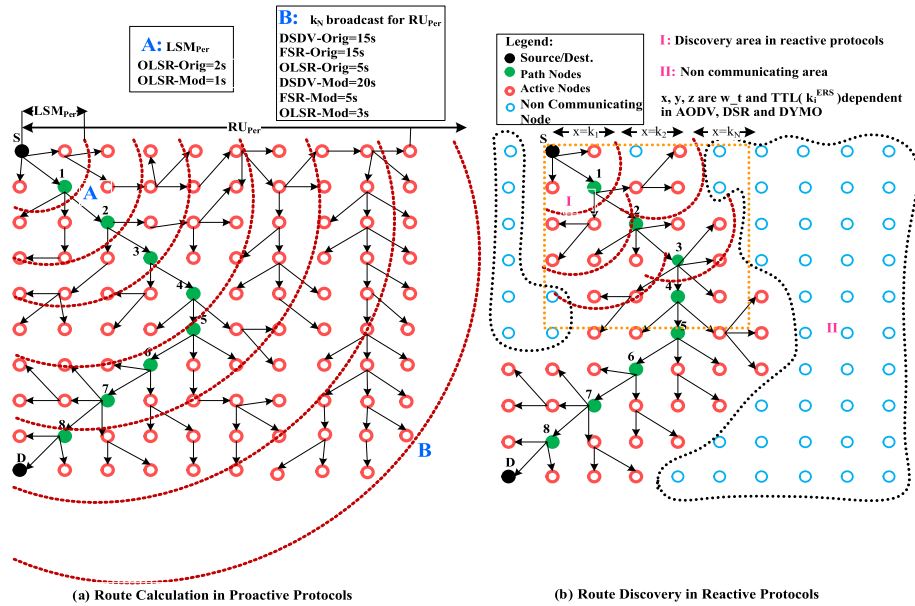


FIGURE 3. Route discovery process in different protocols that use flooding strategy.

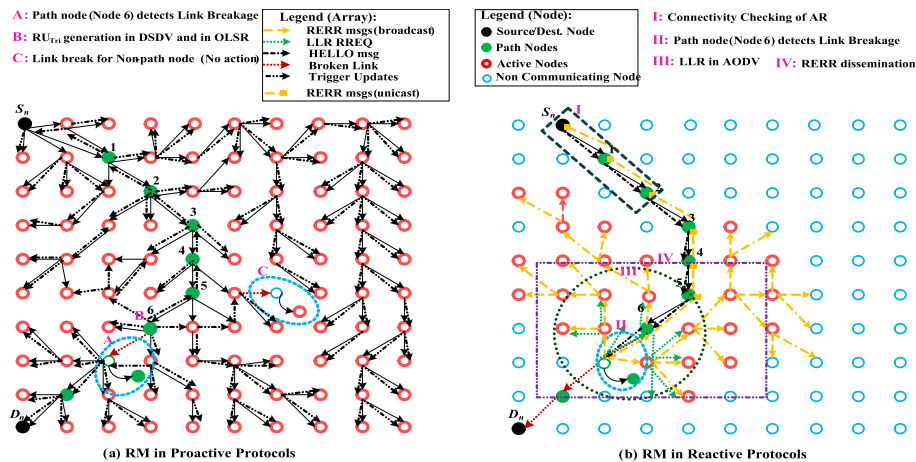


FIGURE 4. Route maintenance process in routing protocols.

spread RU_{Tri} ; $CE_{Tri}^{(DSDV)}$. calculated using equation 4 [12].

$$CE_{total}^{(DSDV)} = CE_{Per}^{(DSDV)} + CE_{Tri}^{(DSDV)} \quad (4)$$

Let τ_{NL} denotes network life time and τ_{Per} is the interval to generate RU_{Per} (in the other words, *full dump* period), then $CE_{Per}^{(DSDV)}$ is estimated using equation 5.

$$CE_{Per}^{(DSDV)} = \frac{\tau_{NL}}{\tau_{Per}} \left(CE_{flooding}^{kN} \right) \quad (5)$$

The RU_{Tri} updates are flooded when link breakages happen in AR that cause change in LS of AR and it costs C^{AR} . The triggering cost of DSDV, $C_{Tri}^{(DSDV)}$, is computed using 6.

$$CE_{Tri}^{(DSDV)} = \int_0^{\tau_{NL}} |sgn(C^{AR})| \left(CE_{flooding}^{kN} \right) \quad (6)$$

If, at any instant, the value of $|sgn(C^{AR})|$ becomes 1, then *incremental update* is flooded to notify this change.

Routing latency can increase end-to-end delay while delivering data to the destination. DSDV has the ability to maintain the data for a predefined time, termed as route settling time (τ_{rst}), which enables the selection of the best route. Holding time may also occur during the settling time of DSDV. Moreover, time is spent when updating the routing table with correct route(s) using RU_{Tri} , after detecting the link breakages. It is denoted by τ_{TU} . The total time cost or time spent by DSDV, $CE_{total}^{(DSDV)}$, is determined using equation 7.

$$CT_{total}^{(DSDV)} = \begin{cases} \tau_{rst} + \sum_i^{node} (L)_i & \text{Successful packet delivery} \\ \tau_{rst} + \sum_i^{node} (L)_i + \tau_{TU} & \text{Otherwise} \end{cases} \quad (7)$$

where, $node$ and L denote the total number of nodes in AR and individual link delay in seconds, respectively.

B. ENHANCED DSDV (DSDV-MOD)

To reduce redundant Route Updates (RUs), τ_{rst} and τ_{per} of $DSDV-Orig$ have been modified in this work. We modified the values of τ_{rst} and τ_{per} and changed them from $6s$ to $7s$ and $15s$ to $20s$, respectively. RU_{per} intervals are mentioned in fig. 3(a). These modifications resulted in stabilized routes' advertisement and augmented the RU_{per} intervals, thus reducing the overhead of RUs . It is worth mentioning that the values of τ_{rst} and τ_{per} are modified in such a way that there is rare trade-off in the performance parameters of DSDV-MOD. That is none of the parameters is compromised to achieve any of the other parameters. On the other hand, suppose if we increase τ_{rst} from $6s$ to $15s$, the throughput is increased from 30 to 40% on the cost of delay, which is increased from 20 to 25% . The final selection of τ_{rst} and τ_{per} is the result of in depth and comprehensive study of the protocol followed by the extensive simulations.

IV. TTL-BASED ROUTING APPROACHES

Instead of broadcasting control messages in entire network (as in traditional flooding), some techniques are used to limit $k(i)$. ERS and SR work on the principle of setting TTL values for $k(i)$, which limits the broadcast region.

A. ERS

The search set value, k_i , in ERS is used to form broadcast levels (rings). Different k_i 's are selected by ERS mechanism to perform search, whereas, each k_i is associated with a specific waiting time. ERS strategy reduces the chances of flooding in the entire MANET by gradually increasing the broadcast rings during search process by setting different TTL values of k_i . This results in limiting the search or Route Discovery (RD) coverage area to reduce energy cost, as depicted in fig. 3(b). The cost of ring i by setting k_i , in terms of routing control packets per ring, $CE_k^{ERS}(i)$ depends on the value of TTL . The average degree for individual k_i in perspective of TTL in ERS, $d_{avg}^{k_i}$, depends on $d_f^{k_i}$. In fig. 2, $d_f^{k_i}$ is analogous to TTL values and waiting time in ERS. The average degree, $d_{avg}^{k_i}$, is computed using equation 8, taken from [12].

$$d_{avg}^{k_i} = \frac{1}{TTL(k_i)} \sum_{i=1}^{TTL(k_i)} d_f[i] \quad \text{for ERS} \quad (8)$$

However, it may be required to repeat these attempts by varying k_i during ERS until D_n is discovered. Let M is the maximum number of k_i , then total CE consumed during ERS, $CE_{total_k}^{ERS}(M)$ is given by equation 9.

$$CE_{total_k}^{ERS}(M) = \sum_{i=1}^M CE_k^{ERS}(i) \quad (9)$$

where, $CE_k^{ERS}(i)$ is calculated using equation 10.

$$CE_k^{ERS}(i) = \begin{cases} P_s d_{avg}^{k_i} & \text{if } TTL(k_i) = 1, \\ P_s d_{avg}^{k_i} + d_{avg}^{k_i} \sum_{TTL=1}^{TTL(k_i)-1} & \\ (P_s)^{TTL+1} \prod_{j=1}^{TTL} d_f[j] & \text{Otherwise.} \end{cases} \quad (10)$$

B. ERS IN ORIGINAL AODV, DSR AND DYMO (AODV-ORIG, DSR-ORIG AND DYMO-ORIG)

AODV, DSR and DYMO routing protocols are modeled in this section to analyze the effect of ERS in each. These protocols use ERS for RD by broadcasting Route REQuest (RREQ) messages from S_n . S_n may receive Route REPlies (RREPs) from D_n or from Relay node R_n . In case of RREPs form R_n , alternative route for the desired destination is accessed from RT of R_n 's. Such type of RREPs are known as gratuitous RREPs (Grat. RREPs). The destination generates the Destination. RREPs $Dest$. RREPs itself. These RREPs generated by all three reactive protocols); whereas, Grat. RREPs are not generated in DYMO. TTL_values and waiting time for k_i are used by all of the above mentioned routing protocols according to their own search strategies. Energy cost of the selected reactive protocols, $CE_{(k-RD)}^{ERS-rp}(rrep)$, for $k_{rrep} = 1$ and onward, is estimated using equation 11.

$$CE_{(k-RD)}^{ERS}(rrep) = \begin{cases} CE_k^{ERS}(rrep) + \sum_{n=1}^{n_{rrep}} (RREP)_n & \text{if } TTL(k_{rrep}) = 1, \\ \sum_{i=1}^{k_{rrep}} CE_k^{ERS}(i) + \sum_{n=1}^{n_{rrep}} (RREP)_n & \text{Otherwise.} \end{cases} \quad (11)$$

where, k_{rrep} denotes the search set (ring) that generates RREPs and is unicasted to S_n .

During RD, k_i search varies with respect to particular protocol's strategy, k_{rrep} denotes the ring that generates RREP (either Grat. RREP or Dest. RREP). The value of M varies according to success or failure of RD.

As k_i for AODV, DSR and DYMO are different, therefore, CE of the respective protocol will also be different. In DSR, basic ERS mechanism is adopted, wherein every attempt after failure of previous attempt results in doubling of previous TTL along with waiting time in the next k_i . The procedure of basic ERS is explained in algorithm 2. In AODV and DYMO, TTL_START value is assigned to $TTL(k_1)$, and then is incremented by two for $TTL(k_2)$ and $TTL(k_3)$. When TTL reaches to its threshold value, $TTL_THRESHOLD$, $TTL(k_4)$ is set to 35 in AODV and 10 in DYMO (according to $TTL_NETDIAMETER$ [2], [5]), whereas, $TTL(k_5)$ is set to 70 and 20 for AODV and DYMO, respectively ($NET_TRAVERSAL$ in [2] and [5]).

Algorithm 2 Basic ERS Mechanism

```

1: Preconditions: Mode  $\in$  {source_node( $S_n$ ), intermedi-
   ate_node ( $I_n$ ), destination_node ( $D_n$ )}
2: while  $S_n$  starts ERS do
3:   set ( $TTL\_VALUE \leftarrow 1$  AND waiting_time  $\leftarrow \tau$ )
4:   broadcasts RREQ (b_RREQ)
5:   for all b_RREQ do
6:     if ( $I_n = D_n$ ) then
7:        $D_n$  generates RREP to  $S_n$ , RDP successful, stop
       ERS
8:     else
9:       if no RREP receives to S AND  $\tau$  expires then
10:        if  $TTL\_VALUE\_TTL \leq MAX\_VALUE$  then
11:          go to step 6
12:        else
13:          stop search set
14:        end if
15:      else
16:        stop ERS
17:      end if
18:    end if
19:  end for
20: end while

```

In case of AODV, links in AR are locally repaired after detecting breakages. The respective energy cost for this repairing process, $CE_{k-RM}^{(ERS)}(llr)$, is computed using equation 12.

$$CE_{k-RM}^{(ERS)}(llr) = P_s d_{avg}^{k_{llr}} + d_{avg}^{k_{llr}} \sum_{TTL=1}^{TTL(k_{llr})-1} (P_s)^{TTL+1} \prod_{j=1}^{TTL} d_f[j] \tag{12}$$

where, k_{llr} represents the search set for Local Link Repair (LLR) activity, as shown in fig. 4(b). TTL value for k_{llr} is calculated using $LOCAL_ADD_TTL$ (value equal to 2) and MIN_REPAIR_TTL (the last known hop-count to the destination). It also depends upon the TTL value of k_{llr} . In large networks, successful and accurate LLR calculation is required, because the chances of route re-discovery are reduced and more bandwidth is utilized. The $TTL(k_{llr})$ is calculated using equation 13.

$$TTL(k_{llr}) = \max(MIN_REPAIR_TTL, 0.5 \times \#hops) + LOCAL_ADD_TTL \tag{13}$$

where $\#hops$ is the number of hops to the sender of the currently undeliverable data packet. The local route repair attempts are often invisible to the originating node, and have $TTL \geq MIN_REPAIR_TTL + LOCAL_ADD_TTL$.

The CT of reactive protocols depends on waiting time for k_i . During RD, waiting time associated with each $k(i)$ is different in AODV, DSR and DYMO. Let τ_1 is the time obtained as $2 \times NODE_TRAVERSAL_TIME$, τ_2 is the value of $BUFFER_TIME_OUT$, and τ is the waiting time of DSR

for *NonPropagating RREQ* [4]. Time cost of these routing protocols, $CT_{k-RD}^{(ERS)}(k)$, is calculated using equation 14, taken from [12].

$$CT_{k-RD}^{(ERS)}(k) = \begin{cases} \sum_{k_i=1}^{k_{rrep}} \tau_1(TTL(k_i) + \tau_2) & \text{for AODV and DYMO,} \\ \sum_{k_i=1}^{k_{rrep}} 2^{k_i-1} \times \tau & \text{for DSR.} \end{cases} \tag{14}$$

As k_i based on TTL value for LLR is also performed during Route Maintenance (RM) process, therefore it has some time cost. Let $CT_{k-llr}^{(AODV)}$ denotes the time spent during LLR , then it is computed using equation 15.

$$CT_{llr}^{AODV} = \tau_1(TTL(k_{llr})) + \tau_2 \tag{15}$$

In the next sub-section, we discuss the enhancements proposed for the selected reactive protocols to optimize routing overhead.

C. ERS IN ENHANCED AODV, DSR, AND DYMO (AODV-Mod, DSR-Mod, AND DYMO-Mod)

Routing latency as well as routing overhead solely depend on corresponding TTL values and waiting times [12]. To optimize the routing overhead, we set $TTL(k_1)$ and $TTL(k_2)$ to 3 and 6, respectively, in *AODV-Mod*, *DSR-Mod* and *DYMO-Mod*. Moreover, $TTL(k_3)$ values in *AODV-Mod* and *DYMO-Mod* are taken to be 9, respectively. Whereas, $TTL_NETDIAMETER$ and $TTL_NETTRAVESAL$ of *DYMO-Orig* is changed to 35 and 70, respectively. On the other hand, TAP_CACHE_SIZE of *DSR-Mod* is adjusted to 256 and $LOCAL_ADD_TTL$ of *AODV-Mod* is reduced to 1.

D. SR IN ORIGINAL FSR (FSR-ORIG)

In SR search strategy, different scopes based on TTL values, are selected to exchange routing information. To reduce overhead of routing updates, ‘‘graded’’ frequency technique is associated with each scope. The basic principle behind the working of SR is that entries corresponding to nodes within the smaller scopes, which have less TTL value, are propagated with highest frequency compared to the larger scopes. CE of any i^{th} scope, $CE_S(i)$, with TTL value associated with $TTL(S(i))$ is calculated using equation 16, taken from [12].

$$CE_S(i) = P_s d_{avg}^S(i) + d_{avg}^S(i) \sum_{TTL=1}^{TTL(S(i))} (P_s)^{TTL+1} \prod_{j=1}^{TTL} d_f[j] \tag{16}$$

where, $d_{avg}^S(i)$ is the average degree of scope i . A protocol sets its scope levels, the overall energy cost of these scopes up to maximum number of scope levels M_S in SR,

Algorithm 3 Scope Routing

```

1: Preconditions: Update_Intervals={periodic for
   IntraScope( $\tau_{IAS}$ ), periodic for InterScope  $\tau_{IES}$ }
2: begin
3: if update_interval= $\tau_{IAS}$  then
4:   for all  $n_{IAS} \in N_{IAS}$  do
5:     set  $TTL \leftarrow 2$ 
6:     broadcast link state INFO
7:   end for
8: else
9:   update_interval= $\tau_{IES}$ 
10:  for all  $n_{IES} \in N_{IES}$  do
11:    set  $TTL \leftarrow 255$ 
12:    broadcast link state INFO
13:  end for
14: end if

```

$CE_{SR}^{M_S}$, is estimated using equation 17.

$$CE_{SR}^{M_S} = \sum_{i=1}^{M_S} CE_S(i) \quad (17)$$

FSR and Global State Routing (GSR) use SR strategy. We select FSR because its concept originates from GSR. In FSR, a moderate approach is taken as it uses only periodic updates (LSM_{Per} and RU_{Per}), as shown in fig. 4(a), and uses two scope levels; *IntraScope* (IAS) and *InterScope* (IES) [6].

Energy cost for IAS is CE_{IAS} with TTL value of 2 for $k_s(IAS)$ and for IES is CE_{IAS} with TTL value of 255 for $k_s(IES)$. The periodic propagation in different scopes can be seen from fig. 2 and can be understood from algorithm 3. The energy cost for SR technique in FSR $CE_{SR}^{(FSR)}$ is expressed using equation 18

$$CE_{SR}^{(FSR)} = \frac{\tau_{NL}}{\tau_{IAS}} \times CE_{IAS} + \frac{\tau_{NL}}{\tau_{IES}} \times CE_{IES} \quad (18)$$

where, τ_{IAS} specifies the periodic interval for IAS and is called *IntraScopeInterval* [6], which is 5s and τ_{IES} represents the periodic interval of IES and known as *InterScopeInterval*, which is by default 15s. Where τ_{NL} shows the periodic updates for the network life time. The values of CE_{IAS} and CE_{IAS} are calculated using equations 19 and 20, respectively.

$$CE_{IAS} = P_s d_{avg}^{IAS} \sum_{TTL=1}^{TTL(k_s(IAS))} (P_s)^{TTL+1} \prod_{j=1}^{TTL} d_f[j] \quad (19)$$

$$CE_{IES} = P_s d_{avg}^{IES} \sum_{TTL=1}^{TTL(k_s(IES))} (P_s)^{TTL+1} \prod_{j=1}^{TTL} d_f[j] \quad (20)$$

To clearly understand the relationship between scope levels with their frequencies in SR, refer algorithm 3. The values used in this algorithm are taken from [6].

Algorithm 4 MPRs Flooding

```

1: begin
2:  $N_1(S_n) \leftarrow$  set of 1st_hop neighbors of  $S_n$ 
3:  $N_2(S_n) \leftarrow$  set of 2nd_hop neighbors of  $S_n$ 
4: for all  $n \in N$  do
5:    $S_n \leftarrow n$ 
6:   start with an empty set of  $MPR(S_n)$ 
7:   for all  $n_1 \in N_1(S_n)$  do
8:     if  $n_1$  has link with  $N_2(S_n)$  then
9:       select  $n_1$  as  $mpr$ 
10:    else
11:      add  $n_1$  as 1st-hop neighbor list
12:    end if
13:    for all  $mpr \in MPR(S_n)$  do
14:      select  $mpr$  with highest degree
15:      if (covers all  $N_2(S_n)$ ) then
16:        stop MPRs selection process
17:         $S_n$  lists  $MPR(S_n)$ 
18:      else
19:        select  $n_1$  with highest degree
20:      end if
21:    end for
22:  end for
23: end for
24: end

```

E. SR IN ENHANCED FSR (FSR-Mod)

In proactive protocols, routes must be updated quickly to maintain accuracy of routes in RT. As, FSR has no such mechanism to update routes after

detecting link breakage, therefore, it needs periodic maintenance with less refresh intervals. In *FSR-Orig*, τ_{IAS} is 5s and τ_{IES} is 15s, which are too large intervals for mobile networks. Therefore, we set τ_{IAS} to 2s and τ_{IAS} to 5s in *FSR-Mod* to increase the frequency of topological information exchange.

V. DEGREE-BASED ROUTING STRATEGY

Degree-based strategy selects multi-point relays in the network based on node degree and reduces the routing control overhead in the network by minimizing duplicate retransmissions in the same region. In this mechanism, each node in the network selects a set of nodes in its 1st-hop neighborhood, known as Multi Point Routing set (MPR mechanism is shown in fig. 2), that provides connectivity to the 2nd-hop neighbors. Detailed functionality of MPR mechanism is depicted in algorithm 4. The energy cost CE of MPRs, $CE_{mpr}^{k_N}$, is computed using equation 21.

$$CE_{mpr}^{(k_N)} = P_s d_{avg}^{mpr} \sum_{TTL=1}^{TTL(k_N)} (P_s)^{TTL+1} \prod_{j=1}^T TLD_f^{mpr}[j] \quad (21)$$

Here, we define the MPR forwarding degree d_f^{mpr} as described in [12]: if x denotes a network node, then $N(x)$ gives the set of 1st-hop neighbors, whereas, $N^2(x)$ gives its 2nd-hop neighbors. Similarly, $N(x)$ lies in the neighboring

region of x , such that $x \in N(x)$. If y is the 1^{st} -hop neighbor of x , then it means that y is directly linked with x or in other words, they both are immediate neighbors. Furthermore, if both S and T denote collection of nodes, then x covers T iff T is either a subset or a superset of S . A set of 1^{st} -hop neighbors, $S \subseteq N(x)$, is MPR of node x if it wraps $N^2(x)$, or equivalently $\cup_{y \in N(x)} N(y) - N(x) \subseteq \cup_{y \in S} N(y)$. Hence, MPR forwarding degree, d_f^{mpr} , is calculated using equation 22.

$$\cup_{y \in N(x)} N(y) - N(x) \subseteq \cup_{y \in S} N(y) \quad (22)$$

In fig. 2, $d_f^{mpr}[k_1]$ is 4, and $d_f^{mpr}[k_2]$ is 8.

A. DEGREE-BASED ROUTING IN ORIGINAL OLSR (OLSR-ORIG)

MPR is used in both reactive and proactive protocols as in AODV, OLSR [7], etc. In this work, we just focus on OLSR to analyze the routing approach based upon the degree of nodes. OLSR uses *HELLO* and *Topology Control* (TC) messages during route computation. Let $CE_{(total)}^{(OLSR)}$ represents the total accumulative energy cost of OLSR and is the sum of $CE_{HELLO}^{(OLSR)}$ and $CE_{TC}^{(OLSR)}$, calculated using equation 23.

$$CE_{total}^{(OLSR)} = CE_{HELLO}^{(OLSR)} + CE_{TC}^{(OLSR)} \quad (23)$$

OLSR generates RU_{Tri} only to maintain the updated routes. The change of interval for transmission of routing is in direct proportion with the status of MPR. If MPR status remains the same, then TC messages are transmitted in a predefined interval. OLSR triggers routing update messages when a change in status of MPR nodes occurs, as shown in fig. 4(a). Let C_s^{MPR} represents this change, then the energy cost for transmitting TC after default interval, $CE_{TC}^{(OLSR)}$, is given using equation 24.

$$CE_{TC}^{(OLSR)} = \int_{\tau_{NS}}^{\tau_{NL}} / \text{sgn}(C_s^{mpr}) / CE_{flooding}^{kN} + \frac{\tau_{NL}}{\tau_{TC-def}} CE_{mpr}^{kN} \quad (24)$$

where, τ_{NS} is the network start time and τ_{TC-def} is TC default time period of OLSR.

B. DEGREE-BASED ROUTING IN ENHANCED OLSR (OLSR-Mod)

In enhanced version of OLSR, we enhanced the RU_{LSM} and RU_{Per} intervals. In *OLSR-Mod*, τ_{HELLO} is set to $1s$ and τ_{TC} is set to $3s$, as RU_{Per} interval for *OLSR-Mod* and *OLSR-Orig* are shown in fig. 3(a).

In the upcoming section, the simulation results of the original protocols and their enhanced versions are discussed. Thee different parameters are used for the performance evaluation of these protocols; *throughput*, *E2ED* and *NRL*.

VI. SIMULATION RESULTS

The performance of the modeled framework of original and enhanced routing protocols AODV, DSDV, DSR, DYMO, FSR and OLSR is measured through simulations in NS-2.

The values of different simulation parameters and results of simulations for reactive protocols are taken from [12]. The Constant Bit Rate (CBR) traffic sources having packet size of 512 bytes and Random Waypoint mobility model are considered in the simulations. Nodes are dispersed in square network area of $1000m \times 1000m$ having $2Mbps$ bandwidth links to carry out communication. Three performance parameters: *throughput*, *E2ED* and *NRL* are chosen for the performance evaluation of the selected protocols.

It is worth mentioning that all of the selected protocols are enhanced in such a way that there is rare trade-off in the performance parameters of the modified protocols. That is none of the parameters is compromised to achieve any of the other parameters.

Also, the enhancements made in the protocols do not have any impact their overall complexity. Moreover, these modifications are not just the changes in the configuration parameters. Not only all of the six routing protocols have been studied in depth and compared but also after hundreds of experiments these configurations have been finalized.

For mobility analysis, two different cases are considered, which are:

- 50 nodes having pause times ranging from 0s to 900s are simulated at a constant speed of 30m/s and
- nodes having different densities, ranging from 10 to 100, are simulated at a constant speed of 15m/s having a uniform pause time of 2s.

Moreover, different data flows with varying data rate (*packets/s*) e.g. 2, 4, 8, 16 and 32 *packets/s*, are considered to examine efficiency of the protocols.

A. THROUGHPUT

It is defined as the amount of data exchanged successfully among source-destination pairs during specified simulation time (network life time). A protocol needs quick convergence to operate efficiently during high mobilities.

1) GENERAL BEHAVIOR OF REACTIVE PROTOCOLS REGARDING THROUGHPUT

As discussed earlier, different k_i 's affect the efficiency of ERS in AODV, DSR and DYMO protocols appreciably. In AODV, k_i s are reduced due to timely-based route checking in RT to make available correct route information. The routes are shortened and routing delays are reduced, using *Grat. RREPs* as compared to DSR, which has no such strategy as shown in fig. 5(a) at 0s, 100s and 200s pause times. *Grat. RREPs* provide quick paths and increase *throughput* of AODV in high mobilities.

In DSR, due to large *TAP_CACHE_SIZE* of 1024 and longer time intervals for routes' storage, RC contains stale routes. Moreover, the value of *RouteCacheTimeout* is 300s in DSR. Incorrect RCing in high mobility scenarios generates noisy and erroneous route information in DSR. The reason is the absence of such mechanisms, which are able to delete stale routes; except RERR messages. In result,

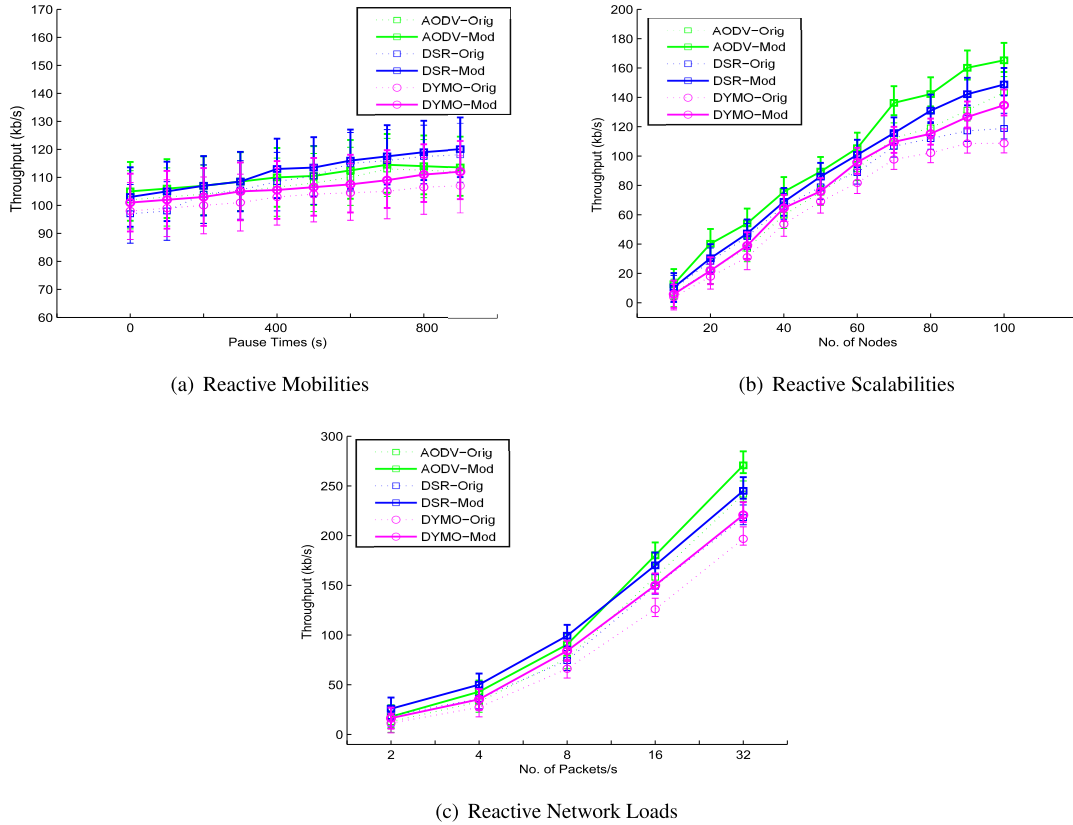


FIGURE 5. Network Throughput Achieved using Original and Enhanced Reactive Protocols.

it increases drop rates. Similarly, quick and efficient route repairing is required; once, the link breakage is detected, for re-establishment of paths by maintaining the broken links. Therefore, *LLR* (refer fig. 4(b)) makes AODV more adaptable to high mobility rate as compared to the other reactive protocols because it diminishes the chances of route re-discoveries.

DSR exhibits highest *throughput* than AODV and DYMO in moderate and immobile scenarios (as depicted in fig. 5(b)), because of *RCing* during *RD* process and *PS* for route maintenance makes end-to-end path calculation quick by reducing k_i . Different mechanisms are used in various protocols like *Grat. RREPs* are used in AODV and DSR, *LLR* is used in AODV and *RCing* and *PSing* are used in DSR. However, DYMO lacks in providing such a mechanism; therefore, there exists lack of optimization to limit k_{rrep} . AODV outperforms among all selected protocols in case of dense network; network with large number of nodes (refer fig. 5(b)) or with high data traffic (refer fig. 5(c)). AODV exhibits one major feature: *LLR*, which increases its suitability in scenarios having high scalabilities and high traffic rates. It is due to the reduction in routing latency, as depicted in fig. 5(c). On the other hand, DSR performs better in low scalable network scenario by reducing k_i through *PSing* and *RCing*, however, due to dissemination of source routing information in dense networks, more *Grat. RREPs* increase the *CE*. This results in increased drop rates. Same behavior of DSR is also noticed in fig. 5(c), the case of varying data flow rates.

2) REACTIVE THROUGHPUT: ORIGINAL AND ENHANCED BEHAVIOR

In case of varying dynamicity, having pause times ranging from $0s$ to $200s$ (with step size of $100s$), *AODV-Orig* attains increased *throughput* than *DSR-Orig*, as shown in fig. 6. The reason is the storage of stale routes during *RC* in *DSR-Orig*. On the contrary, both *AODV-Orig* and *AODV-Mod* check for the *RTs* having valid time and refrain from the usage of invalid routes. Moreover, an efficient repair mechanism for route re-establishment, known as *LLR*, is used. Furthermore, *DSR-Mod* results in high *throughput* as compared to *AODV-Orig*, due to 25% decrease in the actual size of *RC*. This also helps *DSR-Mod* to eliminate outdated routes and to make the initial ring size k_1 of *DSR-Mod* (having *TTL* value equal to 3) discover the routes faster as compared to *DSR-Orig* (fig. 6).

Similarly, reduction in *RING_TRAVERSAL_TIME* of 25ms makes *AODV-Mod* more efficient in high mobilities and the *DYMO-Orig*, among reactive protocols, achieves overall less *throughput*. In DYMO, *Grat. RREPs*, *LLR*, *PSing*, *RCing*, and dissemination of source route information collectively result in increased drop rate as compared to other protocols. Same as that of *AODV-Mod*, low *RING_TRAVERSAL_TIME* in *DYMO-Mod* increases its *throughput* because of quick convergence as compared to *DYMO-Orig* for varying mobilities, as shown in fig. 6.

For varying network sizes, *AODV-Mod* produces higher *throughput*, as *TTL_START* ($TTL(k_1)$), *TTL_INCREMENT*

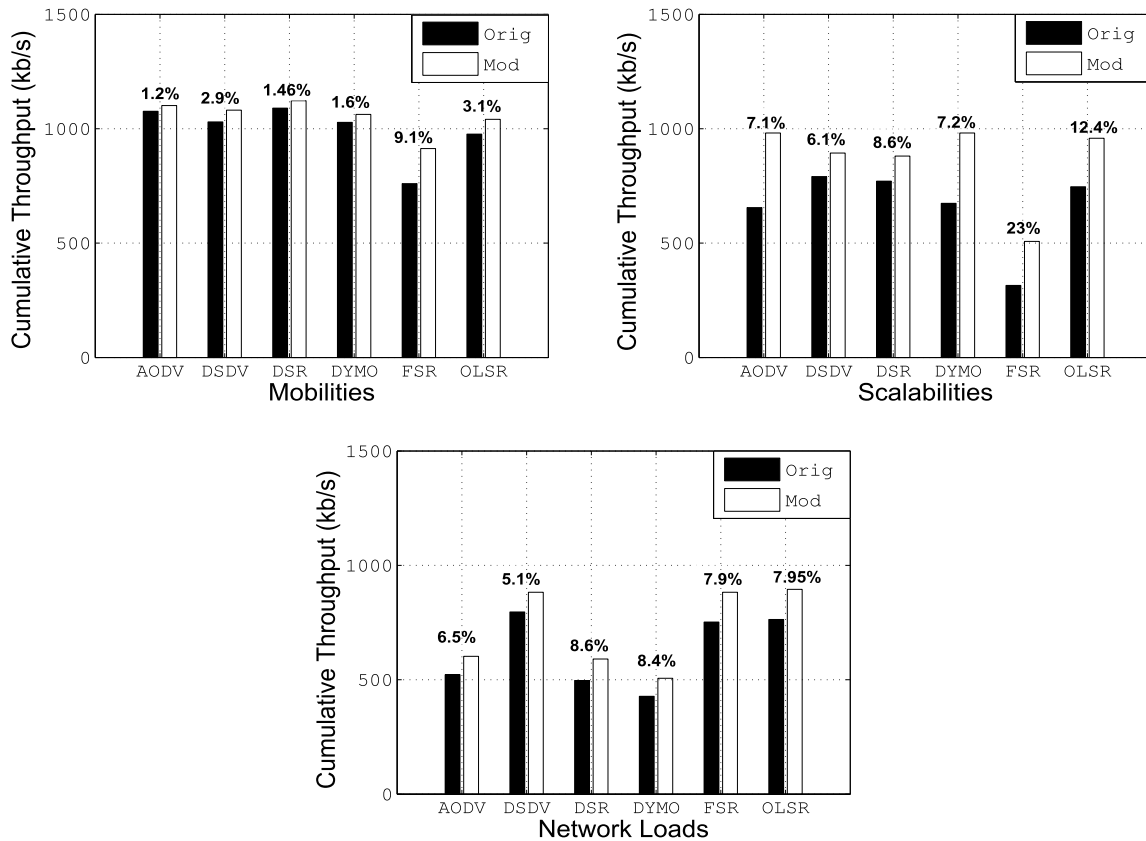


FIGURE 6. Comparison of Throughput Achieved using Original and Enhanced Protocols.

($TTL(k_2)$) and $TTL_THRESHOLD(TTL(k_3))$ are set to 3, 3, and 9. By quick search through large value of $TTL(k_i)$ along with reduction of $RING_TRAVERSAL_TIME$, AODV becomes more scalable for high densities as well as network loads, as depicted in fig. 6. Same thing happens in $DYMO-Mod$ unlike $DYMO-Orig$, where two more k_i s: ($TTL(k_5) = 30$) and $TTL(k_6)=60$) are introduced. The addition of two more k_i s increases the scalability of the system. The increase in initial ring size $TTL(k_1)=3$ increases the scalability of $DSR-Mod$ and enables it to perform better in scenarios having 80, 90, and 100 nodes, respectively. Fig. 5(b) and fig. 6 illustrate this thing.

3) GENERAL BEHAVIOR OF PROACTIVE ROUTING PROTOCOLS REGARDING THROUGHPUT

Fig. 7(a) shows that DSDV has the highest throughput in a network with high mobilities as compared to other proactive protocols. This is due to generation of RU_{Tri} based on C_S^{AR} and delay, that advertise the routes which are in state of transition and cause damping irregularities in the RTs . The number of rebroadcasts of the routes having same sequence numbers is lessened by slowing down the advertising process of un-stabilized routes, which further improves the accuracy. Moreover, it also results in increase of throughput for DSDV for different mobility rates. On the other hand, a gradual

decrease in throughput is observed due to low converging rate of OLSR in high mobility scenarios. The reason is that increasing mobility increases C_S^{mpr} and causes flooding. Although RU_{Tri} 's are generated by both OLSR and DSDV, however, τ_{LSM} is high for OLSR as compared to LSM_{Per} interval of DSDV because of MAC layer notification. Moreover, $2 \times HELLO_LOSS$ parameter decides generation of RU_{Tri} in OLSR, which is approximately 4s. In result, OLSR has low convergence behavior in high mobility scenarios. As RU_{Tri} 's are absent in FSR, therefore, it is less convergent to mobilities as compared to OLSR and DSDV, as portrayed in fig. 7(a).

Among proactive protocols, FSR produces highest throughput for varying traffic rates, as shown in fig. 7(c). OLSR, on other hand, is suitable for networks having variations in their sizes, as depicted in fig. 7(b). In medium and high data traffic, FSR outperforms other protocols because it introduces SRs with graded frequencies, which minimize the routing overhead and works better even when available bandwidth is low. Consequently, it achieves more throughput in case of high data traffic rate and reduces routing overhead. Although, DSDV uses NPDUs to reduce routing control overhead of flooding; however, RU_{Per} as well as RU_{Tri} degrade its performance. MPRs in OLSR provide more optimizations in larger scalabilities, as shown in fig. 7(b), because it reduces

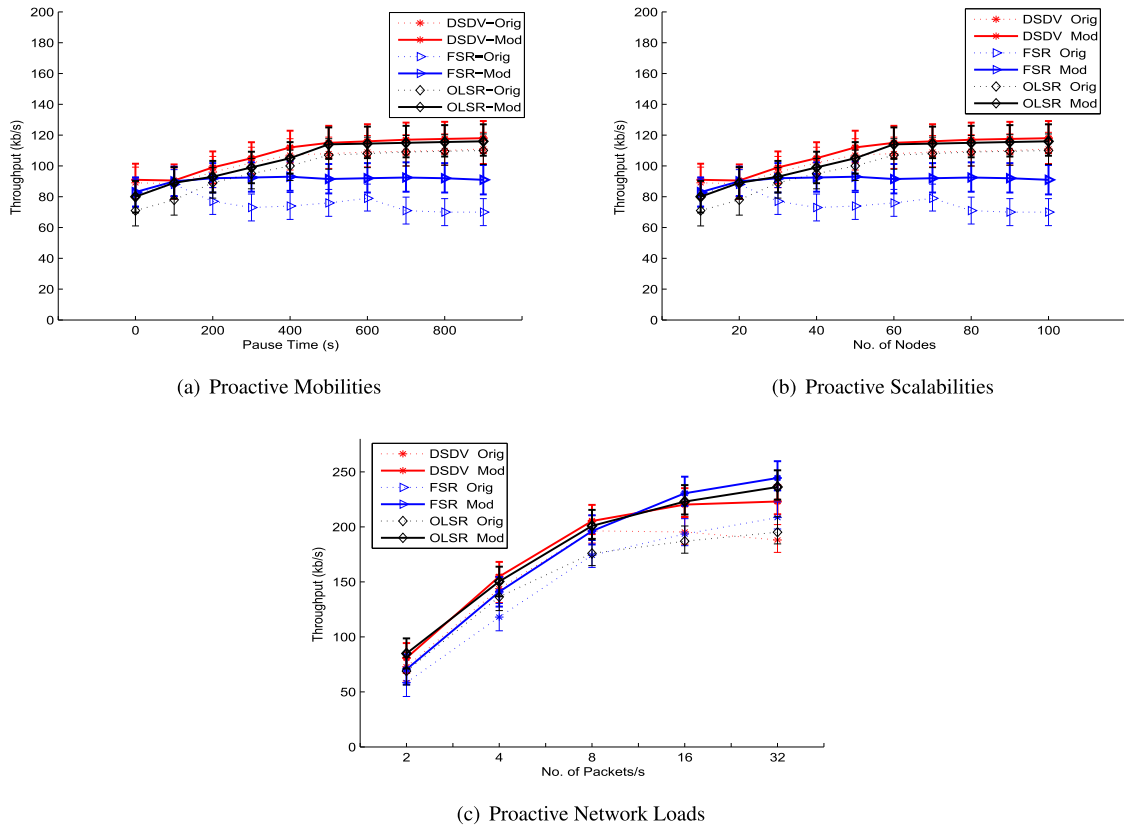


FIGURE 7. Network Throughput Achieved using Original and Enhanced Proactive Protocols.

node degree through d_f^{mpr} and thus achieves high efficiency. The comparative degree of flooding and MPRs can easily be seen in fig. 2.

4) PROACTIVE THROUGHPUT: ORIGINAL AND MODIFIED BEHAVIOR

Shortening the update intervals, τ_{HELLO} and τ_{TC} messages, make *OLSR-Mod* more convergent as compared to *OLSR-Orig*, as shown in fig. 3(a) and fig. 6. Therefore, increase in τ_{rst} along with MAC layer notification of DSDV as compared to τ_{HELLO} of OLSR (in *OLSR-Orig* and *OLSR-Mod*) collectively result the highest throughput attained by *DSDV-Mod* among all proactive protocols. Similarly to *OLSR-Mod*, we reduce topological information exchange intervals in *FSR-Mod* by decreasing the value of τ_{IAS} and τ_{IES} , which results high throughput as compared to *FSR-Orig*, refer fig. 6, whereas absence of RU_{Tri} makes it less efficient for high mobilities.

Simulation of different scalabilities traffic rates, $2s$ pause time, also introduces some mobility, resulting frequent updates in MPRs. Therefore, *OLSR-Mod* outperforms *OLSR-Orig* in terms of scalability as well as traffic rates as depicted in fig. 7(b), 7(c) and in fig. 6. Same as that of OLSR, by increasing frequencies in exchanging information, *FSR-Mod* gives better results in selected scalabilities as well as network flows as shown in fig. 7(a), 7(b), 7(c) and in fig. 6.

On the other hand, changes in *DSDV-Mod* result less number of RU_{Tri} due to more stabilizations and thus reduce the bandwidth consumption cost of flooding exchange. Thus, *DSDV-Mod* produces less drop rate by enhancing the protocol efficiency as compared to *DSDV-Orig* (fig. 7(a), 7(b), 7(c) and in fig. 6).

B. E2ED

E2ED is the total time a packet takes to reach D_n from S_n . In this section, we simulate and analyze the *E2ED* performance of the above said routing protocols for varying pause times, network sizes and data traffic rates.

1) GENERAL BEHAVIOR OF PROTOCOLS REGARDING *E2ED*

For varying mobilities as well as varying network sizes, DYMO attains the lowest routing latency as demonstrated in fig. 8(a) and 8(b) because it only uses ERS (CT_{ERS}) to find suitable routes and results in less delay. Initial assessment of the values of RC in DSR and RT in AODV prior to RD through ERS causes delay in processing of both protocols. Although, CT of DYMO and AODV are calculated similarly as in eq. (14), however, LLR of AODV along with $TTL(k_5)$ and $TTL(k_6)$ are greater in AODV as compared to DYMO which results in less routing latency for DYMO. At higher mobilities, DSR suffers with higher *E2ED* (refer fig. 8(a)) because it looks for the desired route in RC first. Upon failure

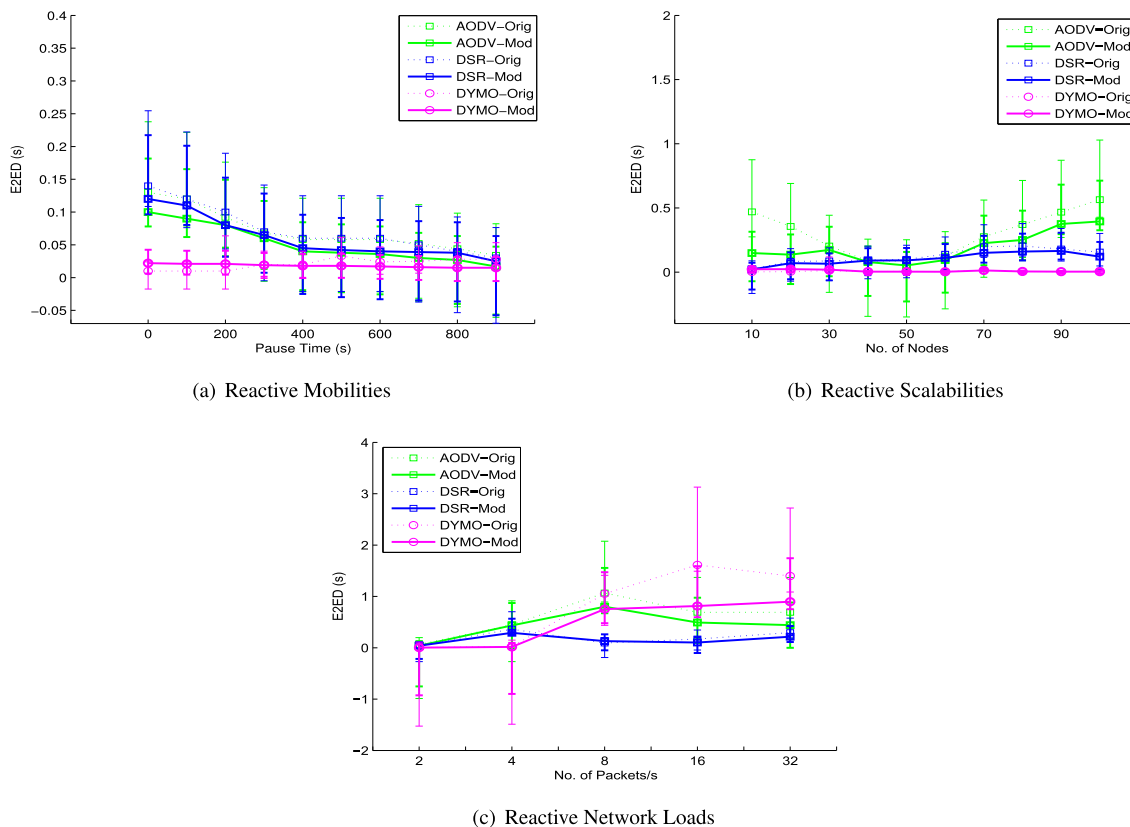


FIGURE 8. Average Delay Faced by Network with Original and Enhanced Reactive Protocols.

of searching the desired route, RD is initiated. Since, *LLR* is not implemented in DSR; therefore, it exhibits less *E2ED* as compared to AODV. Moreover, in moderate and high mobility scenarios, route search failure occurs frequently in RC, which leads to increased delay in DSR. Higher *E2EDs* are observed by reactive protocols, when considering medium to high network loads, as depicted in fig. 8(c). Diverse effects are observed in scenarios having different data packet rates and node densities in AODV and DSR, when *Grat. RREPs* are used. However, this strategy is not used for DYMO, which leads to reduction in delay for small data traffic rates and increases the latency in case of high data rates. Fig. 8(c) illustrates this thing. On the other hand, for different scalability cases, absence of *Grat. RREPs* keeps the value of *E2ED* to its lowest in DYMO protocol, refer fig. 8(b). Similarly, PS and *Grat. RREPs* help in reducing the system halts in different traffic scenarios for DSR, ranging from moderate to high. Initial validation of the RC values is encouraged in place of initiating simple RD process based upon ERS calculation, because it increases the delay in DSR for larger networks as compared to DYMO, refer fig. 8(b). Owing to the presence of LLR process, AODV possesses the maximum value of *E2ED* in all scalability scenarios. However, a decrease in latency is observed due to the decision based upon the congestion of *LLR*; 16 packs/s and 32 packs/s compared to 8 packs/s, refer fig. 8(c).

2) REACTIVE *E2ED*: ORIGINAL AND MODIFIED BEHAVIOR

DYMO-Mod produces the high *E2EDs* as compared to *DYMO-Orig* for higher mobilities and network flows. It uses two additional rings k_5 and k_6 , to achieve efficiency in high scalabilities, while these two rings introduce routing delay in case of highly mobile network with large data traffic rate. The quick search due to decrease in *RING_TRAVERSAL_TIME* along with increase in first three k_i 's of both *AODV-Mod* and *DYMO-Mod*, minimizes delay in contrast to *AODV-Orig* and *DYMO-Orig* (refer fig. 8(a),8(b),8(c) and fig. 9). Presence of stale routes enhances the delay through production of *Grat. RREPs* and increase in route re-discoveries in *DSR-Orig*. In *DSR-Mod*, the large *TTL* values in k_i affects other ring sizes drastically by reducing the routing latency. Moreover, they also avoid stale routes in small cache size and reduce the route re-discovery delay. Overall, *DSR-Mod* has less *E2ED* compared to *DSR-Orig*, as shown in fig. 9. In low scalabilities, due to the increase in path lengths, the delay increases via *LLR*. The route latency is shortened by decrementing the *LOCAL_ADD_TTL* value during repairing process in *AODV-Mod*, as obvious from fig. 8(b).

3) GENERAL BEHAVIOR OF PROACTIVE ROUTING PROTOCOL REGARDING *E2ED*

DSDV produces the highest *E2ED* among all proactive protocols working in scenarios having moderate to low mobilities

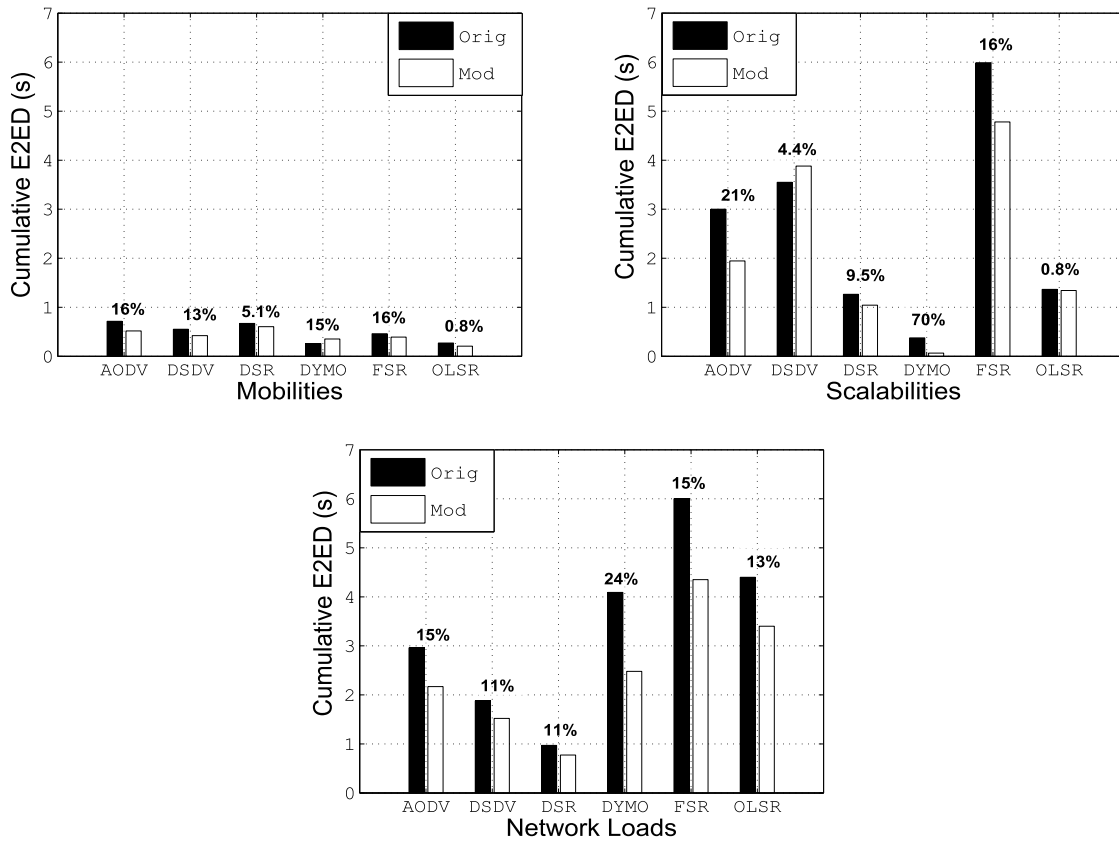


FIGURE 9. Comparison of Delay in Original and Enhanced Protocols.

because of τ_{rst} , as evident from fig. 10(a). Furthermore, there is an intentional delay in advertisement of the unstabilized routes, in order to achieve reduction in the number of rebroadcasts of possible route entries. In FSR, LSM_{Per} information is collected from MAC layer notification, increased link breakages in high mobilities increase round trip time of data packets due to absence of RU_{Tri} . Thus, routes are only re-established through RU_{Per} after τ_{IAS} and τ_{IES} as shown in fig. 10(a).

OLSR has the lowest routing latency as compared to other protocols for varying mobilities and network size, because of the highest frequency of topological information exchange, as depicted in fig. 10(a) and 10(b). In high mobilities, OLSR results more delay as compared to low mobilities, as in OLSR, RU_{Tri} 's are generated after confirming link breakages from HELLO messages through expiration of HELLO_LOSS (2) whereas, HELLO_INTERVAL is also in seconds to check the connectivity. Thus, delay in detecting link breakage introduces latency in updates of RT entries, therefore causes delay in rapidly changing topological environment (fig. 10(a) at 0s, 100s, 200s and 300s pause times). In all scalabilities, shortest interval of RU_{Tri} along more optimizations through MPRs incurs low latency, as exchange of TC messages through MPRs only, reduces retransmission latencies. As we consider 2s of pause times, therefore C_s^{mpr} increases routing update

interval due to stabilization of MPRs from RU_{Tri} , thus causing more E2ED in high densities, as portrayed in fig. 10(b). DSDV attains the lowest E2ED for the high data traffic rate due to quick convergence and delayed advertisement provides stabilized and long lived routes (fig. 10(c)). The highest E2ED is noticed for FSR in fig. 10(c), as broken routes are updated only through next RU_{Per} after τ_{IAS} and τ_{IES} , therefore stable routes are not available for long time, thus RTT of a single data packet is much higher for more network loads.

4) PROACTIVE E2ED: ORIGINAL AND MODIFIED BEHAVIOR
 Decreasing the value of update intervals of both OLSR-Mod and FSR-Mod reduces overall E2ED in all selected scenarios. Whereas, stabilized routes of DSDV-Mod and increased value of τ_{rst} decrease its delay in all network scenarios, as can be seen from fig. 10(a), 10(b), and 10(c). In OLSR-Mod, we reduce RU interval for both $\tau_{HELLO}^{(OLSR)}$ and $\tau_{TC}^{(OLSR)}$, which results more stabilization of MPRs and quick link sensing of neighbors. Thus, decrease in E2ED values by reducing the chances of redundant TC messages, and enabling quick maintenance in RT entries. Same as OLSR-Mod, in FSR-Mod, RU_{Per} for both IES and IAS are frequently exchanged thus routes are updated frequently in RT and are provided with low routing latencies as compared to FSR-Orig (as shown in fig. 9).

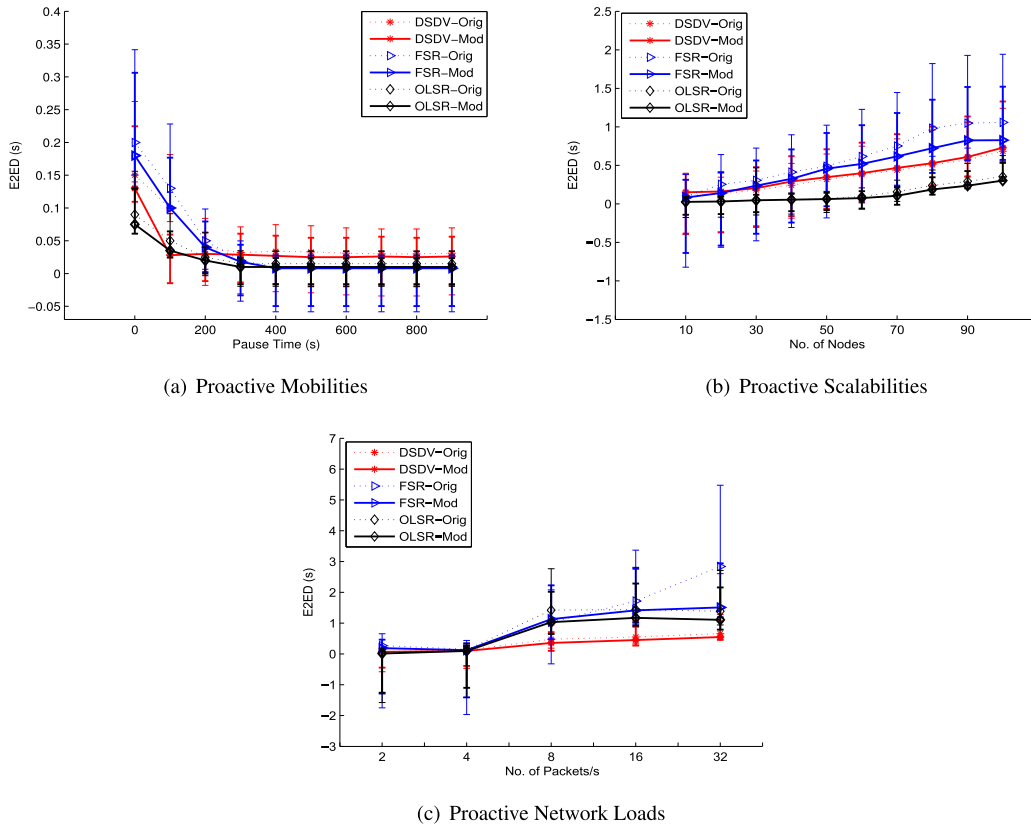


FIGURE 10. Average Delay Faced by Network with Original and Enhanced Proactive Protocols.

C. NRL

It is the number of routing packets transmitted for successful reception of data packets at destination(s).

1) GENERAL BEHAVIOR OF REACTIVE PROTOCOLS REGARDING NRL

In reactive protocols, CE (in terms of control packets) depends on number of k_i 's in RD during ERS and on the mechanisms used to reduce CE of route re-discoveries. ERS is used in other routing protocols as well like AODV, DSR and DYMO. However, different TTL values of k_i s in RD affect CE of the respective protocols. The absence of *Grat. RREPs* in DYMO leads to high TTL_VALUE of k_{rrep} . Therefore, it incurs maximum routing overhead as compared to other reactive protocols in all mobilities and scalabilities (refer fig. 11(a) and 11(b)). On the contrary, less number of routing packets are produced in DSR *RCing* and *PSing*, (as can be seen from fig. 11(a)). The reason is the reduction in TTL_VALUE of k_{rrep} in promiscuous listening mode. Moreover, DSR relies on MAC layer notifications for *LSM* after establishment of ARs unlike DYMO and AODV. In high mobilities with low pause times, reactive protocols generate more control packets as compared to moderate and low mobilities with more pause times, because CE of RM process in high link breakage augments control packets and disseminates of more RERR messages. Increase in number

of *Grat. RREPs* due to high populations also increase routing overhead. Scenarios exhibiting moderate to high population and traffic rates possess less routing load for DYMO (refer fig. 11(b) and 11(c)) as compared to DSR and AODV. AODV attains the maximum routing load due to *LLR* and generation of *HELLO* messages to ensure proper connectivity of AR on network layer.

2) REACTIVE NRL: ORIGINAL AND MODIFIED BEHAVIOR

In *AODV-Mod*, we increase TTL_VALUES of k_1 , k_2 and k_3 . This change effects the number of control packets because CE of any protocol depends on TTL_VALUE of k_i in ERS as depicted in fig. 12. Quick search in initial levels of ERS reduces routing load in mobilities as well as in traffic rate scenarios. We have also changed k_1 size of DSR along with reduction in TAP_CACHE_SIZE . Both of these changes in *DSR-Mod* reduce CE due to reduction in *Grat. RREPs* generation. In all mobilities, moderate and high scalabilities, and in all traffic loads in fig. 12, *DSR-Mod* generates less control packet as compared to *DSR-Orig*. Also modification in initial rings of *DYMO-Mod* along with $TTL_NET_DIAMETER$ and $TTL_NET_TRAVERSAL$ values lowers CE by providing quick search and less number of k_i s for those D_n which are at more distance, as compared to routing overhead of *DYMO-Orig*. One common noticeable behavior of reactive protocols after modifications are made is increase in the

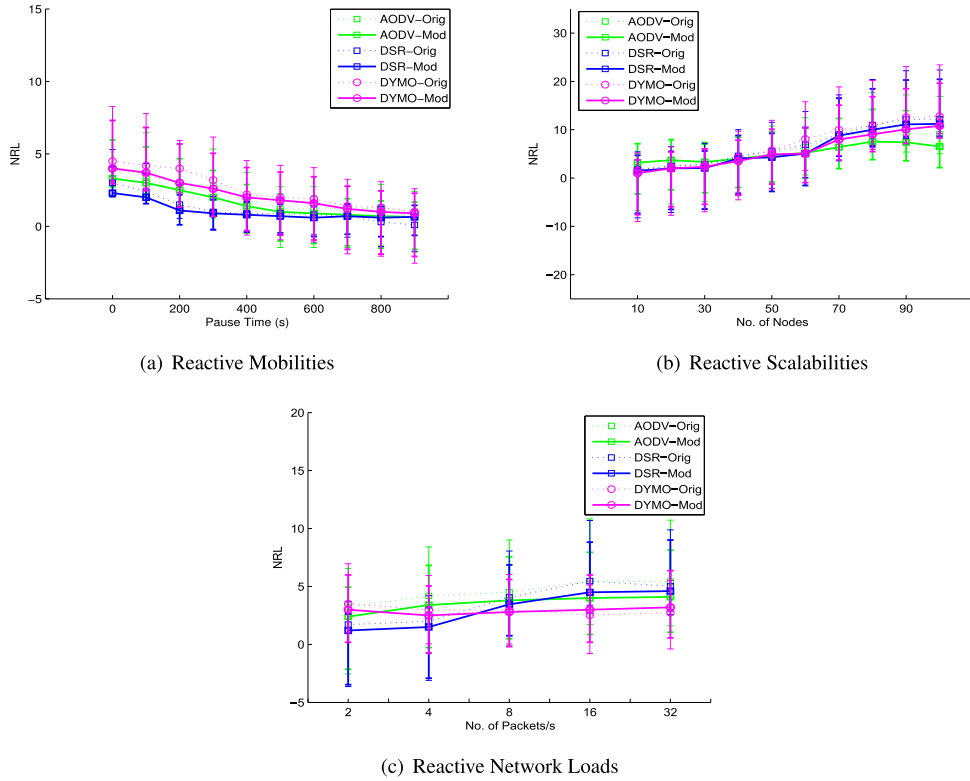


FIGURE 11. Routing Overhead Produced by Network with Original and Enhanced Reactive Protocols.

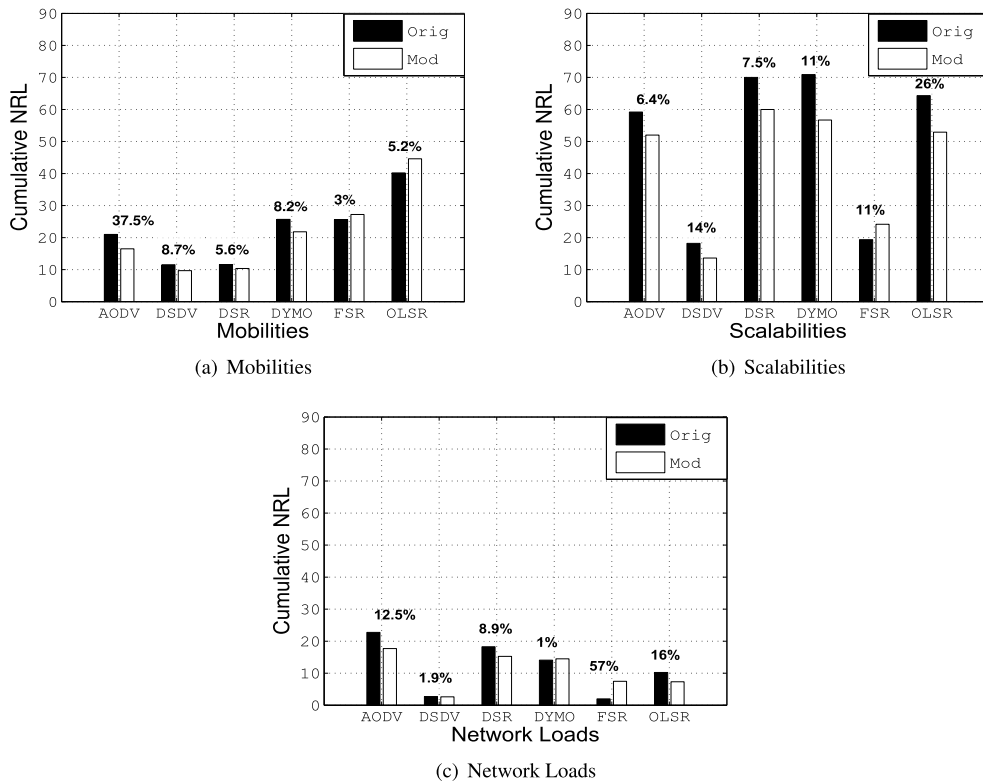


FIGURE 12. Routing Overhead Produced by Original and Enhanced Protocols.

routing load in scenarios having less scalability, where destination nodes are in smaller diameters of S_n s. As we have

modified TTL_VALUES for k_1 and k_2 and assign 3 and 6 values, respectively for all protocols, thus, these changes

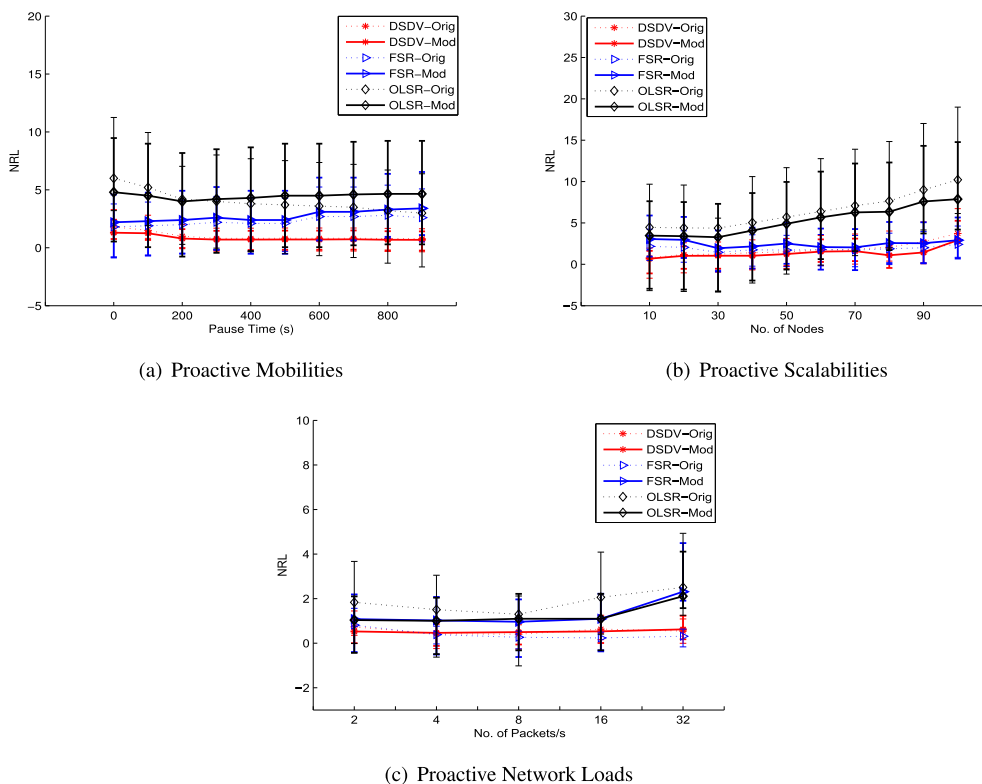


FIGURE 13. Routing Overhead Produced by Network with Original and Enhanced Proactive Protocols.

increase routing load, in fig. 11(b) and fig. 12 at 10, 20 and 30 nodes.

3) GENERAL BEHAVIOR OF PROACTIVE PROTOCOLS REGARDING NRL

Fig. 13(a), 13(b) and 13(c), show that OLSR produces highest routing load as compared to DSDV and FSR. OLSR’s update intervals for TC messages is more than other selected proactive protocols (given in fig. 3(a)); therefore, it consumes more CE. HELLO messages are also generated on network layer for neighbor sensing and for MPRs’ computations unlike FSR and DSDV (rely on MAC layer ACK). Moreover, RU_{Tri} are absent in FSR; whereas, they are used in DSDV and OLSR. In OLSR, C_s^{mpr} causes RU_{Tri} through TC messages, whereas, RU_{Tri} are generated only when link among AR breaks therefore OLSR’s routing load is less when compared with DSDV. The lowest NRL is produced by DSDV in all mobilities as well as in low and medium scalabilities, because, RU_{Tri} are produced in less number for small number of ARs (as shown in fig. 13(a)). Moreover, RU of incremental and periodic dumps through NPDUs help in reducing the routing overhead. As compared to full dump period of DSDV, FSR generates more routing load as compared to DSDV, as portrayed in fig. 12.

4) PROACTIVE NRL: ORIGINAL AND MODIFIED BEHAVIOR

After increasing τ_{rst} value, more stabilization is achieved in DSDV-Mod by lowering the generation of RU_{Tri} and

producing less NRL as compared to DSDV-Orig, as shown in fig. 12 and 13.

Although in OLSR-Mod, RU and LSM exchange intervals are less, however, in all scalabilities and in all traffic loads OLSR-Mod generate less number of control packets as compared to OLSR-Orig. The reason for such behavior of OLSR-Mod in fig. 12 is because more stability of MPRs is achieved due to frequent updates, thus, reducing node degree in high scalabilities, and decreasing RU_{Tri} in high data traffic. On the other hand, OLSR-Mod produces more routing overhead in low pause times, as compared to OLSR-Orig and vice versa for high mobilities, as visualized in fig. 12. In low mobilities, more stabilization of MPRs is achieved with lowest frequency of updates and in high mobilities high frequency is required to update MPRs to avoid redundant TC messages.

As FSR does not generate RU_{Tri} , therefore, increase in τ_{IAS} and τ_{IES} , increase frequency of RU_{Per} (refer fig. 3(a)). Thus in FSR-Mod, these frequent updates generate more routing load in terms of number of control packets in all scenarios as compared to FSR-Orig, as depicted in fig. 12.

VII. CONCLUSION

In WMNs, indirect communication is needed to exchange information among hosts. Routing protocols play a major role in the cases when two hosts want to exchange packets and they cannot communicate directly. Different routing techniques are employed by routing protocols to find a suitable path between the nodes. These routing strategies are

designed to reduce the bandwidth overhead to enable efficient routing and also to reduce the time required for convergence after topological changes. In this work, we mainly focus on analyzing different routing techniques in different scenarios regarding node mobilities, network densities and data traffic rates. We characterize routing techniques in three categories: 1) traditional flooding, 2) *TTL*-based routing and 3) node degree-based routing. To study these techniques in different protocols, we evaluate and compare flooding in DSDV for traditional flooding, route discovery of AODV, DSR and DYMO to examine *TTL*-based ERS, fish-eye SR of FSR to evaluate *TTL*-based SR and topology control transmission of OLSR to compare MPRs flooding with traditional flooding. A novel contribution of this work is the enhancement in search set values and intervals of routing algorithms to improve their efficiencies. A comparison of selected protocols with their default and enhanced routing algorithms is conducted in NS-2 with the help of three performance metrics: *throughput*, *E2ED* and *NRL*. The results depict that *NRL* helps in reducing delay and overall overhead during the data communication.

REFERENCES

- [1] A. Qayyum, L. Viennot, and A. Laouiti, "Multipoint relaying for flooding broadcast messages in mobile wireless networks," in *Proc. 35th Annu. Hawaii Int. Conf. Syst. Sci.*, 2002, pp. 3866–3875.
- [2] C. Perkins, E. Belding-Royer, and S. Das, "Ad-hoc on-demand distance vector routing," in *Proc. IEEE Workshop Mobile Comput. Syst. Appl. (WMCSA)*, Feb. 1999, pp. 90–100.
- [3] C. E. Perkins and P. Bhagwat, "Highly dynamic destination-sequenced distance-vector routing (DSDV) for mobile computers," *ACM SIGCOMM Comput. Commun. Rev.*, vol. 24, no. 4, pp. 234–244, Oct. 1994.
- [4] D. Johnson, Y. Hu, and D. Maltz, *The Dynamic Source Routing Protocol (DSR) for Mobile Ad Hoc Networks for IPv4*, document RFC4728, 2007, pp. 2–100.
- [5] I. Chakeres and C. E. Perkins, *Dynamic MANET On-demand (DYMO) Routing*, document IETF draft-ietf-manet-dymo-05, 2006.
- [6] M. Gerla, *Fisheye State Routing Protocol (FSR) for Ad Hoc Networks*, document IETF Draft-01, 2000.
- [7] T. Clausen, P. Jacquet, C. Adjih, A. Laouiti, P. Minet, P. Muhlethaler, and L. Viennot, *Optimized Link State Routing Protocol (OLSR)*, document RFC 3626, 2003.
- [8] N. Javaid, R. D. Khan, M. Ilahi, L. Ali, Z. A. Khan, and U. Qasim, "Wireless proactive routing protocols under mobility and scalability constraints," *J. Basic Appl. Sci. Res.*, vol. 3, no. 1, pp. 1187–1200, 2013.
- [9] N. Javaid, A. Bibi, A. Javaid, and S. A. Malik, "Modeling routing overhead generated by wireless proactive routing protocols," in *Proc. IEEE GLOBECOM Workshops (GC Wkshps)*, Dec. 2011, pp. 5–9, doi: [10.1109/GLOCOMW.2011.6162343](https://doi.org/10.1109/GLOCOMW.2011.6162343).
- [10] N. Javaid, A. Bibi, A. Javaid, and S. A. Malik, "Modeling routing overhead generated by wireless reactive routing protocols," in *Proc. 17th Asia-Pacific Conf. Commun.*, Oct. 2011, pp. 631–636.
- [11] N. Javaid, Z. A. Khan, U. Qasim, M. Jamil, M. Ishfaq, and T. A. Alghamdi, "Modeling routing overhead of reactive protocols at link layer and network layer in wireless multihop networks," *Math. Problems Eng.*, vol. 2015, pp. 1–14, Jan. 2015, doi: [10.1155/2015/105245](https://doi.org/10.1155/2015/105245).
- [12] N. Javaid, A. Bibi, S. N. Mohammad, Z. A. Khan, and N. Alrajeh, "Towards optimising routing overhead in wireless multi-hop networks," *Int. J. Ad Hoc Ubiquitous Comput.*, vol. 19, nos. 1–2, p. 4, 2015.
- [13] K. Yu, M. Gidlund, J. Akerberg, and M. Bjorkman, "Performance evaluations and measurements of the REALFLOW routing protocol in wireless industrial networks," *IEEE Trans. Ind. Informat.*, vol. 13, no. 3, pp. 1410–1420, Jun. 2017.
- [14] O. O. Ogundile, M. B. Balogun, O. E. Ijiga, and E. O. Falayi, "Energy-balanced and energy-efficient clustering routing protocol for wireless sensor networks," *IET Commun.*, vol. 13, no. 10, pp. 1449–1457, Jun. 2019.
- [15] X. Li, B. Keegan, F. Mtenzi, T. Weise, and M. Tan, "Energy-efficient load balancing ant based routing algorithm for wireless sensor networks," *IEEE Access*, vol. 7, pp. 113182–113196, 2019.
- [16] A. A. Radwan, T. M. Mahmoud, and E. H. Houssein, "Performance measurement of some mobile ad hoc network routing protocols," *Int. J. Comput. Sci. Issues*, vol. 8, no. 1, p. 107, 2011.
- [17] M. Khalid, F. Ahmad, M. Arshad, W. Khalid, N. Ahmad, and Y. Cao, "E2MR: Energy-efficient multipath routing protocol for underwater wireless sensor networks," *IET Netw.*, vol. 8, no. 5, pp. 321–328, Sep. 2019.
- [18] W. He, "Energy-saving algorithm and simulation of wireless sensor networks based on clustering routing protocol," *IEEE Access*, vol. 7, pp. 172505–172514, 2019.
- [19] S. Anamalamudi, A. R. Sangi, M. Alkathairi, and A. M. Ahmed, "AODV routing protocol for cognitive radio access based Internet of Things (IoT)," *Future Gener. Comput. Syst.*, vol. 83, pp. 228–238, Jun. 2018.
- [20] J. Liu, H. Shen, L. Yu, H. S. Narman, J. Zhai, J. O. Hallstrom, and Y. He, "Characterizing data deliverability of greedy routing in wireless sensor networks," *IEEE Trans. Mobile Comput.*, vol. 17, no. 3, pp. 543–559, Mar. 2018.
- [21] S. Feng, Z. Xiong, D. Niyato, P. Wang, Z. Han, and D. I. Kim, "Joint traffic routing and virtualized security function activation in wireless multihop networks," *IEEE Trans. Veh. Technol.*, vol. 68, no. 9, pp. 9205–9219, Sep. 2019.
- [22] F. Yan, X. Zhang, L. Tao, and H. Zhang, "Network coding-based flooding with a mobile sink in low-duty-cycle wireless sensor networks," *IEEE Trans. Mobile Comput.*, vol. 18, no. 8, pp. 1857–1869, Aug. 2019.
- [23] W. Dong, C. Cao, X. Zhang, and Y. Gao, "Understanding path reconstruction algorithms in multihop wireless networks," *IEEE/ACM Trans. Netw.*, vol. 27, no. 1, pp. 1–14, Feb. 2019.
- [24] A. Sinha, L. Tassiulas, and E. Modiano, "Throughput-optimal broadcast in wireless networks with dynamic topology," *IEEE Trans. Mobile Comput.*, vol. 18, no. 5, pp. 1203–1216, May 2019.
- [25] J. Kuang, B. Xie, and R. Ding, "Bandwidth-based real-time streaming in information-centric hybrid multihop wireless networks," *IEEE Wireless Commun. Lett.*, vol. 8, no. 5, pp. 1386–1389, Oct. 2019.
- [26] H.-S. Kim, S. Kumar, and D. E. Culler, "Thread/OpenThread: A compromise in low-power wireless multihop network architecture for the Internet of Things," *IEEE Commun. Mag.*, vol. 57, no. 7, pp. 55–61, Jul. 2019.
- [27] M. Pióro, A. Tomaszewski, and A. Capone, "Maximization of multicast periodic traffic throughput in multi-hop wireless networks with broadcast transmissions," *Ad Hoc Netw.*, vol. 77, pp. 119–142, Aug. 2018.
- [28] S. B. Shah, Z. Chen, F. Yin, I. U. Khan, and N. Ahmad, "Energy and interoperable aware routing for throughput optimization in clustered IoT-wireless sensor networks," *Future Gener. Comput. Syst.*, vol. 81, pp. 372–381, Apr. 2018.
- [29] A. Ladas, D. G. C., N. Pavlatos, and C. Politis, "A selective multipath routing protocol for ubiquitous networks," *Ad Hoc Netw.*, vol. 77, pp. 95–107, Aug. 2018.
- [30] D. Gao, S. Zhang, F. Zhang, T. He, and J. Zhang, "RowBee: A routing protocol based on cross-technology communication for energy-harvesting wireless sensor networks," *IEEE Access*, vol. 7, pp. 40663–40673, 2019.
- [31] J. Zhang and R. Yan, "Centralized energy-efficient clustering routing protocol for mobile nodes in wireless sensor networks," *IEEE Commun. Lett.*, vol. 23, no. 7, pp. 1215–1218, Jul. 2019.
- [32] S. G. Varghese, C. P. Kurian, V. I. George, A. John, V. Nayak, and A. Upadhyay, "Comparative study of ZigBee topologies for IoT-based lighting automation," *IET Wireless Sensor Syst.*, vol. 9, no. 4, pp. 201–207 Aug. 2019.
- [33] M. Parsinia, Q. Peng, and S. Kumar, "Distributed mode selection for FDD communication in multihop wireless networks," *IEEE Trans. Aerosp. Electron. Syst.*, vol. 55, no. 6, pp. 2921–2937, Dec. 2019.
- [34] H. Al-Shatri, K. Keller, F. Jacobfeuerborn, O. Hinz, and A. Klein, "Eliciting and considering underlay user preferences for data-forwarding in multihop wireless networks," *IEEE Access*, vol. 7, pp. 40052–40067, 2019.
- [35] C. Pu and S. Lim, "A light-weight countermeasure to forwarding misbehavior in wireless sensor networks: Design, analysis, and evaluation," *IEEE Syst. J.*, vol. 12, no. 1, pp. 834–842, Mar. 2018.
- [36] X. Bai, X. Wei, and S. Bai, "Efficient receiver-based flooding in mobile ad hoc networks," *Wireless Netw.*, vol. 26, pp. 17–31, Jun. 2018.
- [37] P. K. Biswas, S. J. Mackey, D. H. Cansever, M. P. Patel, and F. B. Panettieri, "Context-aware smallworld routing for wireless ad-hoc networks," *IEEE Trans. Commun.*, vol. 66, no. 9, pp. 3943–3958, Sep. 2018.
- [38] S. Kafaie, Y. Chen, O. A. Dobre, and M. H. Ahmed, "Joint inter-flow network coding and opportunistic routing in multi-hop wireless mesh networks: A comprehensive survey," *IEEE Commun. Surveys Tuts.*, vol. 20, no. 2, pp. 1014–1035, 2nd Quart., 2018.

- [39] A. Bujari, C. E. Palazzi, and D. Ronzani, "A comparison of stateless position-based packet routing algorithms for FANETs," *IEEE Trans. Mobile Comput.*, vol. 17, no. 11, pp. 2468–2482, Nov. 2018.
- [40] J. Jiang and G. Han, "Routing protocols for unmanned aerial vehicles," *IEEE Commun. Mag.*, vol. 56, no. 1, pp. 58–63, Jan. 2018.
- [41] H.-M. Wang, Y. Zhang, D. Wing Kwan Ng, and M. Ho Lee, "Secure routing with power optimization for ad-hoc networks," *IEEE Trans. Commun.*, vol. 66, no. 10, pp. 4666–4679, Oct. 2018.
- [42] Y.-H. Chen, E. H.-K. Wu, C.-H. Lin, and G.-H. Chen, "Bandwidth-satisfied and coding-aware multicast protocol in MANETs," *IEEE Trans. Mobile Comput.*, vol. 17, no. 8, pp. 1778–1790, Aug. 2018.
- [43] J. Bai, Y. Sun, C. Phillips, and Y. Cao, "Toward constructive relay-based cooperative routing in MANETs," *IEEE Syst. J.*, vol. 12, no. 2, pp. 1743–1754, Jun. 2018.
- [44] M. Saleem, S. Khayam, and M. Farooq, "On performance modeling of ad hoc routing protocols," *EURASIP J. Wireless Commun. Netw.*, vol. 2010, Mar. 2010, Art. no. 373759.



FAHAD AHMAD AL-ZAHRANI received the B.Sc. degree in electrical and computer engineering from Umm Al-Qura University, Mecca, Saudi Arabia, in 1996, the M.S. degree in computer engineering from the Florida Institute of Technology, in 2000, and the Ph.D. degree in computer engineering from Colorado State University, in 2005. From 2011 to 2016, he was the IT Dean with Umm Al-Qura University, and he has had several other responsibilities thereafter. He has taught several computer network courses and supervised related research projects. He is currently an Associate Professor at the Computer Engineering Department, Umm Al-Qura University. His research interests include high-speed network protocols, sensor networks, optical networks, performance evaluation, IoT, and blockchain architecture and performance analysis. He is a member of the International Society for Optical Engineering and the Optical Society of America.

• • •